1966

Analysis of crystal size distributions when growth rate is size dependent

Carl Frank Abegg
Iowa State University

67-5567

ABEGG, Carl Frank, 1939-

ANALYSIS OF CRYSTAL SIZE DISTRIBUTIONS WHEN GROWTH RATE IS SIZE DEPENDENT.

Iowa State University of Science and Technology, Ph.D., 1966
Engineering, chemical

University Microfilms, Inc., Ann Arbor, Michigan

ANALYSIS OF CRYSTAL SIZE DISTRIBUTIONS WHEN GROWTH RATE IS SIZE DEPENDENT

by

Carl Frank Abegg

A Dissertation Submitted to the
Graduate Faculty in Partial Fulfillment of
The Requirements for the Degree of
DOCTOR OF PHILOSOPHY

Major Subject: Chemical Engineering

Approved:

Signature was redacted for privacy.
In Charge of Major Work

Signature was redacted for privacy.
Head of Major Department

Signature was redacted for privacy.
Dean of Graduate College

Iowa State University
Of Science and Technology
Ames, Iowa

1966

TABLE OF CONTENTS

ABSTRACT

In this work, empirical size dependent growth rate models are studied for their effect on the population density distribution from a continuous, mixed suspension, mixed product removal (CMSMPR) crystallizer. The growth rate models, and/or their corresponding population density distributions, are examined for continuity, versatility, convergence of moments, mathematical simplicity, and ability to fit experimental data.

Based on this study, a new empirical size dependent growth rate model is proposed which has properties superior to those of previous models. Experimental steady state data are presented to illustrate the application of the model to actual CMSMPR crystallization systems.

Using a general population balance derived by Randolph and Larson (14), a set of equations are developed for predicting the transient response of the crystal population density distribution to various changes in crystallizer operating conditions. In developing this set of equations, it is assumed that the crystal growth rate can be expressed by the proposed model. The transient equations are numerically solved for step changes in production rate and growth rate.

A step increase in production rate causes an instantaneous shower of nuclei to occur. As time passes, the nuclei which are members of this shower grow into larger crystals, thereby causing transients in the population densities of all crystal sizes. The increase in production rate (decrease in residence time) causes the mass distribution to be shifted in the direction of the smaller crystal sizes. The

general transient behavior for a size dependent growth rate is shown to be the same as that for a growth rate independent of size.

Considering the effect of size on crystal settling velocity, it is hypothesized that a sudden change in the level of agitation of a crystal suspension could effect the degree to which crystal growth rates are influenced by size. The transient equations are solved for a step change in growth rate; the step change is from a growth rate independent of size to a size dependent growth rate. Such a change in growth rate might approximate a growth rate change due to a sudden decrease in the level of agitation. The step change in growth rate is shown to increase the dominant particle size and the variance of the mass distribution.

INTRODUCTION

Any crystallization operation can be thought of as consisting of three basic steps:

1. Achievement of some degree of supersaturation.
2. Formation of crystal nuclei or centers of growth.
3. Growth of the crystals.

In commercial crystallization equipment these three steps occur simultaneously and need to be understood and controlled if a uniform product meeting desired specifications is to be produced.

Randolph and Larson (14) derived a general equation which describes the size distribution of particles in an arbitrary suspension. They solved this equation for the steady state and transient size distributions in a continuous, mixed suspension, mixed product removal (CMSMPR) crystallizer with the assumption that crystal growth rate is independent of crystal size. However, for a number of crystalline materials in mixed suspension crystallizers this assumption does not seem to be valid (2, 3, 4b, 6, 11).

The objective of this work is to investigate the effect of size dependent growth rate models on population density distributions from a CMSMPR crystallizer. The general equation derived by Randolph and Larson (14) will be used to determine these distributions.

PREVIOUS WORK

Nucleation

Although a great deal of experimental work has been done, and numerous theories have been proposed, the actual mechanism of spontaneous nucleation is still uncertain. Mullin (9) gives an excellent review of some of the more important theoretical and experimental work which has been done to elucidate the mechanism.

In a classic experiment, Miers and Isaac (8) heated a solution of sodium nitrate above its saturation point and continuously observed the refractive index of the solution as it cooled to room temperature. They found that, in the absence of solid particles, a definite level of supersaturation needed to be attained before nucleation occurred. By repeating the experiment for different concentrations of sodium nitrate, they were able to establish a supersaturation curve below which no nuclei were formed. This supersaturation curve was found to lie approximately parallel to the saturation curve. Figure 1 illustrates the results of their experiment. Curve DE is the saturation curve, and FG is the supersaturation curve. Region A represents unsaturated solution. Region B is a metastable area of supersaturation in which crystals would grow but no spontaneous nucleation would occur. Region C is an area of spontaneous nucleation.

The performance of similar experiments has shown that the position of the supersaturation curve is greatly affected by the presence of seed crystals and the rate of cooling (19). The fact that the rate of cooling influences the position of the supersaturation curve indicates that a

Figure 1. Schematic representation of supersaturation curve determined by Miers and Isaac (8)

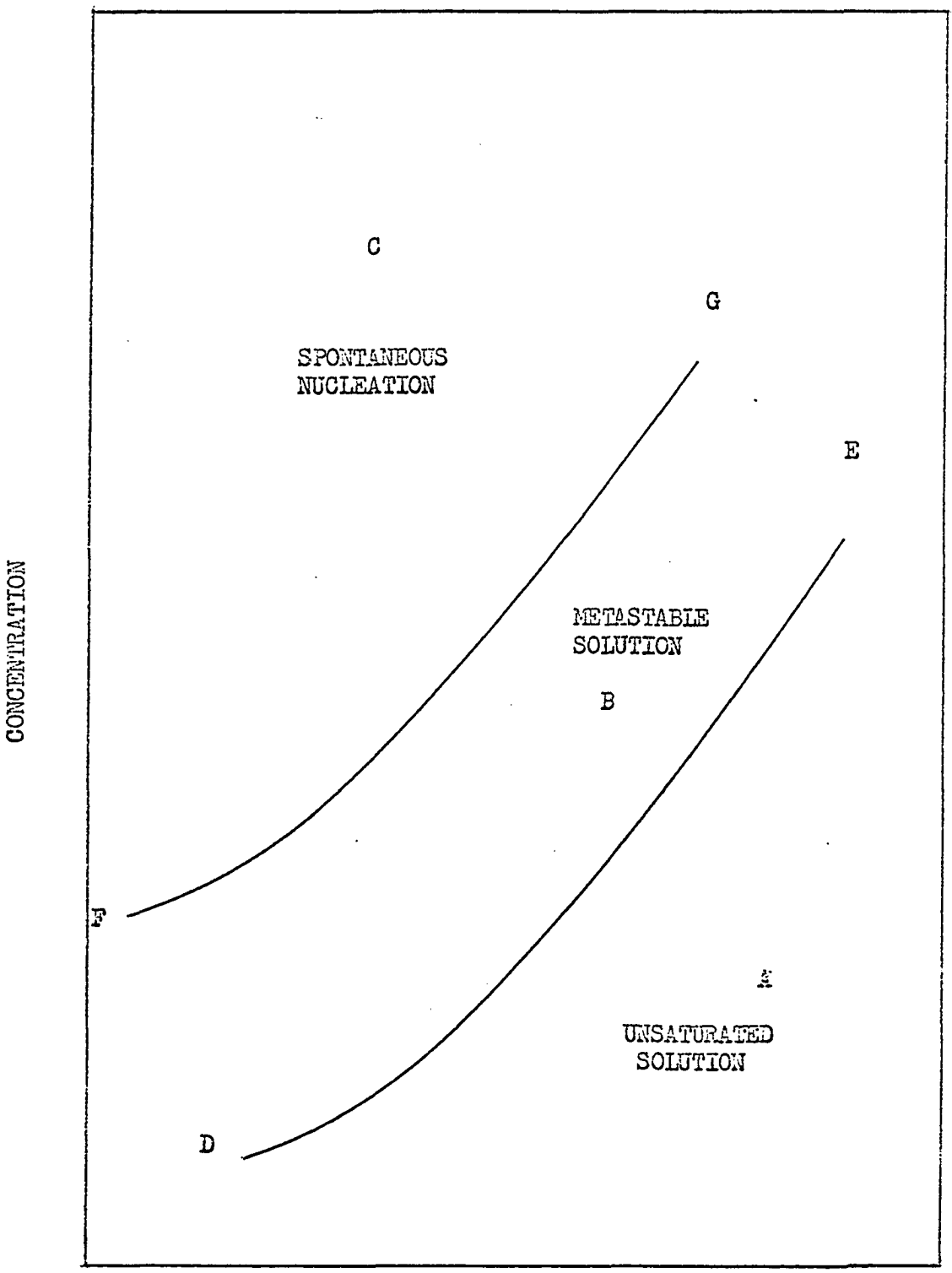
C
G
SPONTANEOUS
NUCLEATION
E
METASTABLE
SOLUTION
B
F
A
UNSATURATED
SOLUTION
D
CONCENTRATION
TEMPERATURE

solution in the metastable region is not indefinitely stable, and a time probability of nucleation exists for supersaturated solutions.

From theoretical considerations, Mullin (9) shows that the amount of work necessary to form a nucleus from a large bulk of solution may be expressed in terms of the supersaturation ratio through the relationship

$$W = \frac{16\pi\sigma^3 \bar{M}^2}{3(R_g T' \rho \ell n \bar{s})^2} \qquad (1)$$

where W = work required to form a nucleus

σ = surface energy per unit area

$\bar{M}$ = solute molecular weight

ρ = solute density

R_g = gas constant

T' = crystallization temperature

$\bar{s} = \frac{c}{c^*}$

c = concentration of solute in the bulk of solution

c^* = equilibrium saturation concentration of the solute

This is an extremely important relationship in that it shows that any supersaturated solution can nucleate spontaneously since the amount of work required is finite. Only for a saturation solution, $\bar{s} = 1$, is an infinite amount of work required. Hence, for any supersaturated solution, the problem reduces to one of supplying the needed amount of energy to the system. Now within any system, the random motion of the molecules causes the energy of various regions of the system to fluctuate about the mean energy level of the system as a whole. Therefore, whenever the energy of a region of the system equals or exceeds the required energy of

nucleation, nuclei will be formed.

According to the Volmer-Becker-Doering theory, the rate of nucleation can be expressed in the form of an Arrhenius velocity equation,

$$\frac{dN^o}{dt} = A'\exp[-\Delta G/R_g T'] \tag{2}$$

where N^o = number of nuclei

A' = constant of proportionality

ΔG = overall excess free energy of the particle,

i.e., the work of nucleation, W

t = time

Combining Equations 1 and 2 one obtains,

$$\frac{dN^o}{dt} = A'\exp\left[-\frac{16\pi\sigma^3 \bar{M}^2}{3R_g^3 (T')^3 \rho^2 (\ell n\, \bar{s})^2}\right] \tag{3}$$

Equation 3 is a rather complex expression which is too unwieldy for most practicle calculations. Very little quantitative data on nucleation rates in CMSMPR crystallizers have been published, but what data do exist show that nucleation rates can often be empirically expressed in terms of a power of supersaturation,

$$\frac{dN^o}{dt} = k_N s^{\alpha} \tag{4}$$

where s is the supersaturation, c-c*, and k_N is a function of fluid properties and operating conditions, such as temperature and degree of agitation (4a,11).

Crystal Growth

As soon as nuclei are formed in a supersaturated solution, they begin

to grow into crystals of visible size. Early theories (9) assumed that crystal growth was a diffusional process and could be described by

$$\frac{dm}{dt} = k_m A(c-c^*) \tag{5}$$

where m = crystal mass

A = crystal surface area

k_m = mass transfer coefficient

On the assumption that solute molecules must diffuse through a thin laminar film of liquid lying adjacent to the crystal surface, Equation 5 can be modified to the form

$$\frac{dm}{dt} = \frac{D}{\delta} A(c-c^*) \tag{6}$$

where D = solute diffusivity

δ = effective thickness of the laminar film

The theory that crystal growth is simply a diffusional process has obvious weaknesses. Since the thickness of the laminar film depends on the relative solid-liquid velocity, Equation 6 implies that no limiting value of growth rate would be achieved as the film thickness is reduced by increased agitation. Also, for the same magnitude in deviation from the saturation concentration, the rates of crystal growth and dissolution should be the same. Experimentally this is not found to be true. Miers (7) made a significant contribution when he found, by refractive index measurements, that for sodium chlorate crystals growing in acqueous solution, the solution in contact with the growing crystal faces was not saturated, but supersaturated. It is now generally held that crystal growth consists of two steps:

(a) the diffusion of solute molecules from the bulk of the solution to the crystal interface, followed by

(b) a surface reaction as the solute molecules arrange themselves into the crystal lattice.

These two steps may be represented by the equations

$$\text{(diffusion)} \qquad \frac{dm}{dt} = \frac{D}{\delta} A(c-c_i) \tag{7}$$

$$\text{(surface reaction)} \qquad \frac{dm}{dt} = k_r A(c_i-c^*) \tag{8}$$

where k_r = reaction rate constant

c_i = solute concentration at the crystal-solution interface.

Equations 7 and 8 may be combined to yield an overall equation for the process,

$$\frac{dm}{dt} = \frac{D}{\delta + D/k_r} A(c-c^*) \tag{9}$$

From Equation 9 it is seen that as $\delta \to 0$, the growth rate approaches an asymptotic value

$$\frac{dm}{dt} = k_r A(c-c^*) \tag{10}$$

and is reaction limited. As $k_r \to \infty$, the growth rate approaches the asymptotic value

$$\frac{dm}{dt} = \frac{D}{\delta} A(c-c^*) \tag{11}$$

and is diffusion limited. Hence, in crystal growth both diffusion and surface reaction can be important, or only one mechanism can be controlling. In studying the crystallization of sodium chloride, Rumford and Bain (15) found the growth rate to be diffusion controlled at temperatures

above 50°C and reaction controlled below this temperature.

It should be noted that in deriving Equation 9, a first-order surface reaction was assumed. The general assumption of a first-order reaction is questionable. Many crystal materials seem to exhibit a first-order surface reaction, while others exhibit higher order reactions (9).

Equation 9 can also be written in the form

$$\frac{dm}{dt} = K\,A(c-c^*) \tag{12}$$

where

$$K = \frac{D}{\delta + D/k_r}$$

and is dependent upon the temperature and relative solid-liquid velocity. The mass of a crystal at any time can be expressed as

$$m = \rho_c\, k_v\, L^3 \tag{13}$$

where ρ_c = crystal density

k_v = a characteristic volumetric shape factor

L = a characteristic dimension of the crystal

From Equation 13

$$\frac{dm}{dt} = 3\,\rho_c\, k_v\, L^2\, \frac{dL}{dt} \tag{14}$$

Since the area of a crystal at any time is proportional to L^2, from Equations 12 and 14 it is seen that the linear growth rate of a crystal can be expressed as

$$r \equiv \frac{dL}{dt} = k_g(c-c^*) = k_g\, s \tag{15}$$

where k_g in general is a function of temperature and the relative crystal-

solution velocity, and the surface reaction is assumed to be first-order.

From experiments performed in a mixed suspension batch crystallizer, McCabe and Stevens (6) found that the growth rate of copper sulfate pentahydrate crystals could be empirically correlated by the equation

$$r = 0.00177 s^{1.8} L^{1.1} \tag{16}$$

To determine if size had a direct influence on the rate at which a crystal grows, crystals of varying size were grown under constant conditions of temperature and supersaturation. By controlling the relative crystal-solution velocities, they were able to correlate the growth rates of crystals of all sizes by the equation,

$$\frac{1}{r} = \frac{1}{r'_o + \beta v} + \frac{1}{r_i} \tag{17}$$

where r = linear growth rate

v = relative crystal-solution velocity

r'_o, β, r_i = constants

Equation 17 shows that as $v \to \infty$, r approaches the asymptotic value, r_i. This is consistent with the theory that crystal growth consists of a diffusion step followed by a surface reaction.

From this investigation it was concluded that crystal growth rate is independent of crystal size per se. The apparent effect of size (Equation 16) results from the larger crystals having a higher settling velocity, and hence, a greater relative crystal-solution velocity.

In an industrial crystallizer, it is much easier to determine the apparent effect of crystal size on the growth rate than it is to measure relative solid-liquid velocities. Hence, a simple practical model for

expressing crystal growth rate would seem to be

$$r = k\, s^a L^b \tag{18}$$

where in general k can be a function of temperature.

An important addition to the recent literature is a paper by Bennett (2) which tabulates crystal size distributions for a wide variety of industrial crystallization equipment and crystal systems. Bennett uses an equation derived by Bransom (3) which incorporates a size-dependent growth rate expression to analyze these data. His analysis shows that for a number of crystal materials in CMSMPR crystallizers, crystal growth rate decreases with crystal size. Unfortunately, the equation derived by Bransom is incorrect. Nevertheless, as Randolph (12) points out, the results obtained by Bennett are qualitatively correct, and show that his data do exhibit crystal growth rates inversely proportional to crystal size. Bennett believes this effect is caused by classification taking place at boiling surfaces where the supersaturation may be considerably higher than in the bulk of the crystal suspension. He assumes that this surface classification dominates the opposite tendency of the large crystals to grow faster because of less diffusion resistance. In any case, it is seen that in general the effect of crystal size on growth rate needs to be taken into account, and non-zero values of b in Equation 18 need to be considered.

An Important CMSMPR Crystallizer Theory

Until 1962, analytical crystallizer theories had dealt only with steady state size distributions. Theories were developed for specific crystallization operations--e.g. mixed suspension or classified product removal crystallizers--and as such, were quite limited in their

applications. Randolph (13) presents a comprehensive historical review of the development of these theories.

In 1962, Randolph and Larson (14) published a general theoretical description of crystallization. They based their development on the concept of population density, n, defined by

$$n = \lim_{\Delta L \to 0} \frac{\Delta N}{\Delta L} \tag{19}$$

where ΔN is the number of crystals contained in a small size range of width ΔL. The derivation used an overall population balance for an arbitrary suspension of particles under unsteady state conditions. The suspension was defined by the following assumptions:

1. The particles in the suspension are small enough and numerous enough to be considered a continuous distribution with respect to size for any given volume element of the suspension.
2. No particle breakage occurs except the possible chipping of a particle into unequal pieces such that the original particle is essentially unchanged in size and the new particles are small enough to be considered nuclei.
3. The suspension occupies a variable volume, V, enclosed by fixed boundaries except for a free gravity surface.
4. The suspension has inputs and outputs which are completely mixed, but the suspension itself need not be mixed.

In the unsteady state case, the accumulation of particles in the suspension equals the input of particles minus the output. Considering

particles in the size range L_1 to L_2, this was mathematically expressed as

$$\frac{d}{dt}\int_V \int_{L_1}^{L_2} \bar{n}dLdV = \int_{L_1}^{L_2} \left[\frac{R_i' \bar{n}_i}{\rho_i} - \frac{R_o' \bar{n}_o}{\rho_o}\right]dL \qquad (20)$$

where $\bar{n}$ is the point population density per unit volume, R' is the suspension input or output flow rate, ρ is the corresponding density, and t is time. By a repeated use of Leibnitz's Rule on the left-hand side of Equation 20 they obtained

$$\frac{d}{dt}\int_V \int_{L_1}^{L_2} \bar{n}dLdV = \int_V \int_{L_1}^{L_2} \left[\frac{\partial \bar{n}}{\partial t} + \frac{\partial}{\partial L}\left(\bar{n}\frac{\partial L}{\partial t}\right)\right] dLdV + \int_{L_1}^{L_2} \frac{dV}{dt}\bar{n}_s\, dL \qquad (21)$$

where the population density at the surface, $\bar{n}_s$, is assumed constant across the entire surface. By interchanging the order of integration and transposing, Equation 20 becomes

$$\int_{L_1}^{L_2} \left\{\int_V \left[\frac{\partial \bar{n}}{\partial t} + \frac{\partial}{\partial L}\left(\bar{n}\frac{\partial L}{\partial t}\right)\right]dV + \bar{n}_s \frac{dV}{dt} - \frac{R_i' \bar{n}_i}{\rho_i} + \frac{R_o' \bar{n}_o}{\rho_o}\right\}dL = 0 \qquad (22)$$

For Equation 22 to be identically zero for an arbitrary size range of particles L_1 to L_2

$$\int_V \left[\frac{\partial \bar{n}}{\partial t} + \frac{\partial}{\partial L}\left(\bar{n}\frac{\partial L}{\partial t}\right)\right]dV + \bar{n}_s \frac{dV}{dt} - \frac{R_i' \bar{n}_i}{\rho_i} + \frac{R_o' \bar{n}_o}{\rho_o} = 0 \qquad (23)$$

Equation 23 is a general population balance for an arbitrary suspension of particles subject to the original four assumptions.

Having derived a general equation, Randolph and Larson (14) considered a continuous, mixed suspension, mixed product removal (CMSMPR) crystallizer operating under the following conditions:

1. The energy input is controlled to maintain a constant suspension density.
2. Constant suspension volume is maintained.
3. Crystal growth rate is independent of crystal size. (This is often referred to as McCabe's ΔL Law.)
4. No particles are present in the input to the crystallizer.

Under these conditions Equation 23 reduces to

$$\frac{\partial n}{\partial t} + r\frac{\partial n}{\partial L} + \frac{n}{T} = 0 \tag{24}$$

where r is the growth rate, $\frac{dL}{dt}$, $n = \bar{n}V$, and $\frac{1}{T} = \frac{R'_o}{\rho_o V}$, the reciprocal drawdown time. (Working independently, Behnken et al. (1) have derived an analogous equation for a process in which particles are growing in a perfectly mixed vessel.)

From conditions 1.) and 2.), the total mass of crystals in the suspension remains constant. By expressing this in the form

$$\frac{dM}{dt} = \frac{d}{dt}\left[\rho_c k_v \int_0^\infty n L^3 \, dL\right] = 0 \tag{25}$$

and using Leibnitz's Rule to differentiate under the integral, the following relationship was derived for the crystal growth rate,

$$r = \frac{k' F}{\int_0^\infty n L^2 \, dL} \tag{26}$$

where F is the feed rate and k' is a constant. Equation 26 shows that there is a dynamic relationship between the size distribution and the crystal growth rate. Since the growth rate also depends on the degree of

supersaturation, as does the nucleation rate, Equation 26 indicates that there is a dynamic relationship between the size distribution and the factors which determine this distribution, namely growth and nucleation rates.

Randolph and Larson (14) put Equation 24 in dimensionless form and solved for steady state distributions, and for transient responses of the size distribution to step changes in feed rate.

To test the theoretical development, Murray and Larson (10) constructed a 5 1/2 liter, salting out, CMSMPR crystallizer. Using the alum-ethanol-water system, they obtained steady state and transient size distribution data which lend experimental support to the theoretical model of Randolph and Larson (14). Using the same crystallization equipment but improved analytical techniques, Timm and Larson (18) have gathered extensive data for three different inorganic crystalline materials which further support the model.

STEADY STATE ANALYSIS

The Selection of a Growth Rate Model

Growth and nucleation kinetics are the two most important factors in determining the product size distribution curve from a crystallizer. Therefore, in order to properly design and operate a crystallizer to produce a desired product distribution, it is advantageous to have mathematical expressions relating nucleation and growth rates to the factors which effect these rates.

In deriving Equation 24, Randolph and Larson (14) assumed that McCabe's ΔL Law, which states that crystal growth rate is independent of crystal size, was obeyed. If the crystal growth rate is sufficiently size dependent, the product size distribution will differ significantly from that predicted by McCabe's ΔL Law. Obviously, in order to correctly predict the size distribution in these cases, a size dependent growth rate expression is required.

The McCabe-Stevens model

As was previously mentioned, McCabe and Stevens (6) found that the growth rate of copper sulfate pentahydrate crystals in a mixed suspension batch crystallizer could be empirically correlated by the equation

$$r(L) = 0.00177 s^{1.8} L^{1.1} \tag{27}$$

Equation 27 suggests the form

$$r(L) = k\, s^{a}\, L^{b} \tag{28}$$

If crystal growth rate is size dependent, Equation 24 is

$$\frac{\partial n}{\partial t} + \frac{\partial}{\partial L}(rn) + \frac{n}{T} = 0 \tag{29}$$

At steady state, $\partial n/\partial t = 0$ and Equation 29 becomes

$$\frac{d}{dL}(r_o n_o) + \frac{n_o}{T_o} = 0 \tag{30}$$

where the subscript "o" indicates steady state. At steady state the supersaturation is constant, so Equation 28 can be written,

$$r_o = k\, s_o^a\, L^b = k_1\, L^b \tag{31}$$

Using this expression for the steady state growth rate, Equation 30 can be integrated to give the steady state population density distributions

$$n_o(L) = n_o^o\, (L^o/L)^b \exp[-RL^{1-b}/1-b + R(L^o)^{1-b}/1-b],\ b \neq 1 \tag{32}$$

$$n_o(L) = n_o^o\, (L^o/L)^{R+1},\ b = 1 \tag{33}$$

where $R = 1/k_1 T_o$, the superscript "o" refers to nuclei, and the boundary condition is $n = n_o^o$ when $L = L^o$.

Setting $n_o^o\, (L^o)^b \exp[R(L^o)^{1-b}/1-b] = K_1$ in Equation 32, and $n_o^o\, (L^o)^{R+1} = K_2$ in Equation 33, these equations can be written as

$$n_o(L) = K_1\, L^{-b} \exp[-RL^{1-b}/1-b],\ b \neq 1 \tag{34}$$

$$n_o(L) = K_2\, L^{-(R+1)},\ b = 1 \tag{35}$$

Having determined the steady state population density distributions generated by a growth rate model having the form of the McCabe-Stevens (M-S) model, it is reasonable to inquire into the applicability of these distributions. A necessary condition for any realistic population density distribution is that moments of the distribution converge, i.e.,

$$I^p \equiv \int_{L_o}^{\infty} n_o(L) \cdot L^p \, dL \quad \text{converges for } p \geq 0 \tag{36}$$

Considering the distribution defined by Equation 34,

$$I^p \equiv K_1 \int_{L_o}^{\infty} L^{p-b} \exp[-RL^{1-b}/1-b] dL \tag{37}$$

A simple test for the convergence of indefinite integrals of the type of Equation 37 is the limit test (16). This test may be written in the form:

1. If $\lim_{x \to \infty} x^c f(x) = A$, then

2. (a) $\int_a^{\infty} f(x)dx < \infty$ if $c > 1$ and A is finite

   (b) $\int_a^{\infty} f(x)dx = \infty$ if $c \leq 1$ and $A \neq 0$,

where the symbols '$< \infty$' and '$= \infty$' denote respectively convergence and divergence of the integrals.

Considering the case $b < 1$ and applying the limit test to Equation 37,

$$\lim_{L \to \infty} K_1 L^{c+p-b} \exp[-RL^{1-b}/1-b] = 0 \text{ , all real } c+p-b \tag{38}$$

Therefore, I^p converges for $b < 1$.

Applying the limit test to Equation 37 for the case $b > 1$,

$$\lim_{L \to \infty} K_1 L^{c+p-b} \exp[-RL^{1-b}/1-b] = \begin{cases} K_1 & , \ c+p-b = 0 \\ 0 & , \ c+p-b < 0 \\ \infty & , \ c+p-b > 0 \end{cases} \tag{39}$$

Hence, I^p converges for $c+p-b \leq 0$, where $b > 1$ and $c > 1$. However, this implies that

$$p \leq b-c \tag{40}$$

Equation 40 sets an upper bound for p. Since the zeroth moment and positive

moments of the distribution have physical meaning, this upper bound should not exist for a realistic population density distribution. Hence, values of $b > 1$ in Equation 34 do not give acceptable distributions.

For $b = 1$,

$$I^p \equiv K_2 \int_{L_o}^{\infty} L^{p-R-1} \, dL < \infty \text{ , for } p < R \tag{41}$$

By definition, $R = 1/k_1 T_o$, and the numerical value of R is determined by the operating conditions of the crystallizer. Hence, from a physical standpoint, the restriction that p be less than R for the convergence of I^p is unrealistic, and the case $b = 1$ is not allowed.

From these results it is seen that only values of $b < 1$ are permitted in the growth rate expression, and the steady state population density distributions generated by the growth rate expression.

The fact that this theoretical result conflicts with that obtained experimentally by McCabe and Stevens, Equation 27, should not be disconcerting. First, Equations 34 and 35 were derived for a continuous crystallizer. In theoretically analyzing size distributions from a continuous crystallizer, one cannot consider a finite size interval, as can be done when analyzing distributions from a batch process. It is, of course, the infinite interval of integration in Equation 36 which presents convergence problems. Second, it was assumed in the derivation of Equations 34 and 35 that no finite particle breakage occurred. In many cases, the degree of agitation and the crystalline material may be such that this assumption is greatly violated. Hence, in an actual crystallization operation, it can be possible for the size exponent in the McCabe-Stevens (M-S) growth

rate model to have values greater than or equal to one. However, in making a theoretical analysis of a continuous crystallizer where it is assumed that no finite particle breakage occurs, one is restricted to considering only values of b less than one in Equation 34.

Equation 34 would be more general and useful if it were written in a dimensionless form such that b would be the only parameter. From the M-S growth rate expression, the size to which a nucleus grows in one steady state draw-down time can be determined.

$$r_o = \frac{dL}{dt} = k\, s_o^a\, L^b = k_1\, L^b \tag{42}$$

Rearranging

$$\frac{dL}{L^b} = k_1\, dt \tag{43}$$

If L_m represents the size to which a nucleus grows at the end of one draw-down time,

$$\int_{L^o}^{L_m} \frac{dL}{L^b} = k_1 \int_o^{T^o} dt \tag{44}$$

Integrating

$$L_m^{1-b} - (L^o)^{1-b} = k_1\, T_o(1-b) \tag{45}$$

In any practical operation of a crystallizer, $L_m >> L^o$.

Since

$$(1-b) > 0 \tag{46}$$

for (1-b) sufficiently large

$$L_m^{1-b} >> (L^o)^{1-b} \tag{47}$$

hence, neglecting $(L^o)^{1-b}$, Equation 45 becomes

$$L_m^{1-b} = k_1 T_o(1-b) = (1-b/R) \tag{48}$$

or

$$L_m = [k_1 T_o(1-b)]^{1/1-b} \tag{49}$$

Introducing the dimensionless variables

$$y = \frac{n}{K_1 L_m^{-b}} , \tag{50}$$

$$x = \frac{L}{L_m} , \tag{51}$$

Equation 34 can be put in the form

$$y_o(x) = x^{-b} \exp[-x^{1-b}] \tag{52}$$

Figure 2 shows the effect of b on the dimensionless steady state population distributions. Considering Equation 52, one sees that

$$\lim_{x \to 0} y_o(x) = \begin{cases} \infty , & b > 0 \\ 1 , & b = 0 \\ 0 , & b < 0 \end{cases} \tag{53}$$

The values of the above limit and Figure 2 illustrate some very serious weaknesses in the M-S growth rate model.

For $b > 0$, the population density increases without bound as $x \to 0$, and it is impossible to determine a finite upper bound on the nuclei density by letting $x = 0$. Since the size of a nucleus is extremely difficult to measure, and so small when compared with the size of any visible crystal, it is often advantageous if one can consider a nucleus to have zero size and determine a finite upper bound for the nuclei density.

For $b < 0$, the population density distribution has an absolute

Figure 2. Steady state dimensionless population density distributions defined by Equation 52

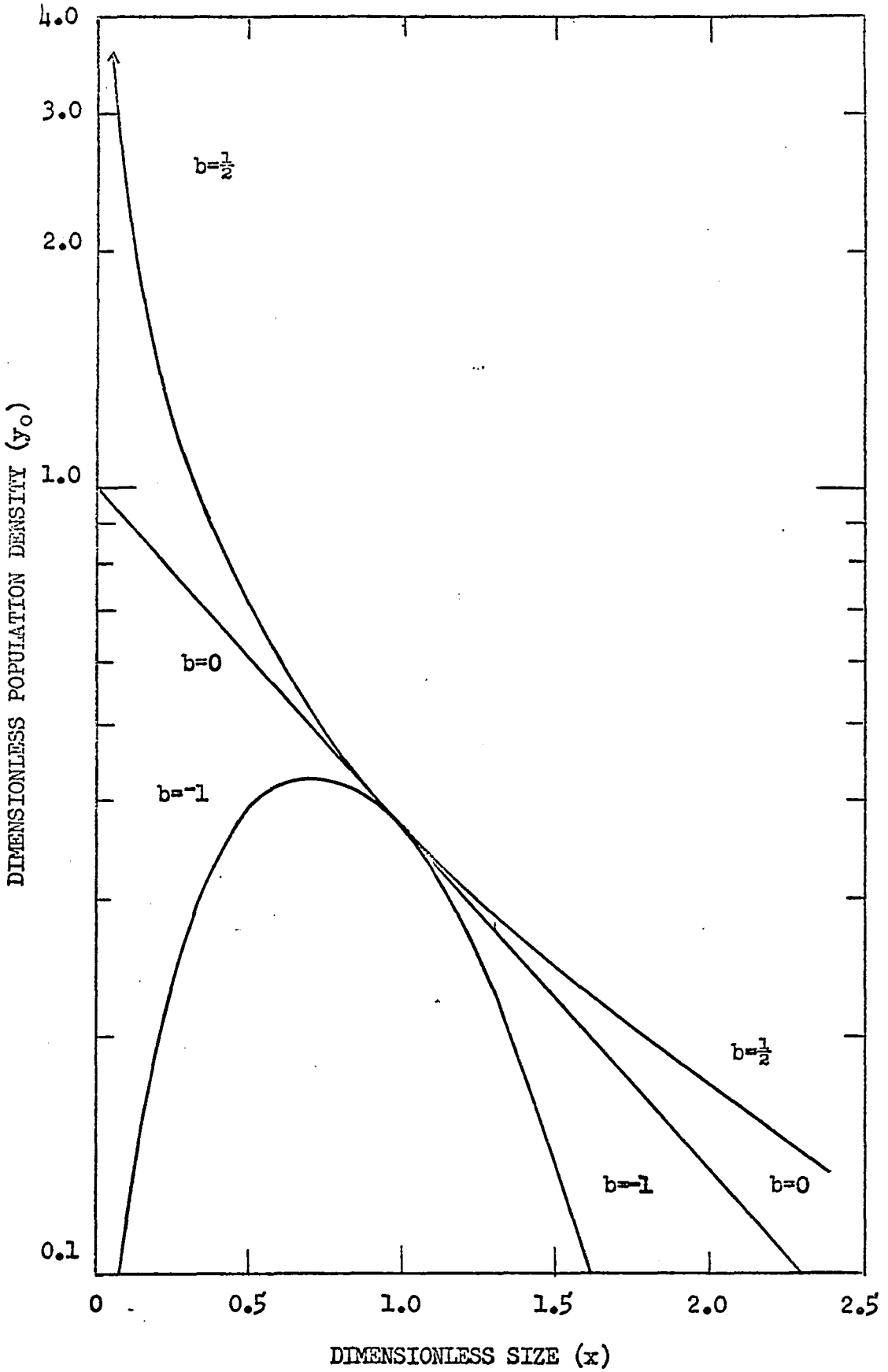
4.0
3.0
2.0
1.0
0.1
0
0.5
1.0
1.5
2.0
2.5
DIMENSIONLESS POPULATION DENSITY (y_o)
DIMENSIONLESS SIZE (x)
b=½
b=0
b=-1
b=-1
b=0
b=½

maximum at some crystal size other than the size of a nucleus. This would not seem to be a very likely situation for an actual distribution from a CMSMPR crystallizer operating with liquid feed inputs. In this type of crystallization operation, all particles in the suspension are present as nuclei at some time in their previous history. Since the probability of a particle remaining in suspension decreases with time, the absolute maximum of a population density distribution generated by a physically acceptable growth rate model should be the nuclei density.

Considering the growth rate model and the population density distribution to be functions of x and b, the model and the population density distribution are discontinuous at the point (x = 0, b = 0). Physically, the existence of such a discontinuity seems completely unreasonable.

A qualitative understanding of the reason for the various limiting values of the population density distribution, Equation 53, can be found by examining the growth rate model. The M-S model at steady state is

$$r_o(L) = k\, s_o^a\, L^b = k_1\, L^b \tag{54}$$

and

$$\lim_{L\to 0} r_o(L) = \lim_{L\to 0} k_1\, L^b = \begin{cases} 0 & , b > 0 \\ k_1 & , b = 0 \\ \infty & , b < 0 \end{cases} \tag{55}$$

From Equation 55 one sees that for b positive, as the crystal size approaches zero, the growth rate approaches zero. Hence, a nucleus having zero size does not grow into a larger crystal, but remains a constant zero size nucleus. As nucleation continues, the number of these nuclei increase without bound. For b negative, as the crystal size approaches zero, the growth rate approaches infinity. In this case, a nucleus of zero size

grows instantaneously into a larger crystal.

The preceding discussion indicates that if it is desired to determine a finite upper bound for the nuclei density by considering a nucleus to have zero size, a growth rate expression is needed which satisfies the condition, $r_o(0) \neq 0,\infty$. The growth rate expression should also be continuous in the region in which it is defined.

Model-I

A simple expression which meets the above requirements is (Model-I),

$$r_o = r_o^o[1 + (\gamma L)^b] \quad , \quad b > 0 \quad , \quad L \geq 0 \tag{56}$$

Substituting Equation 56 into Equation 30, and using the dimensionless variables,

$$y_o = \frac{n_o}{n_o^o} \tag{57}$$

$$x = \gamma L = \frac{L}{r_o^o T_o} \tag{58}$$

the dimensionless differential equation and boundary condition defining the steady state distributions are

$$\frac{dy_o}{dx} = - \frac{(b\, x^{b-1} + 1)y_o}{1 + x^b} \tag{59}$$

where $y_o = 1$ at $x = 0$.

Equation 59 can be rearranged to

$$\frac{dy_o}{y_o} = - \frac{b\, x^{b-1}\, dx}{1 + x^b} - \frac{dx}{1 + x^b} \tag{60}$$

Integrating

$$\ell n\ y_o = -\ \ell n(1+x^b) - \int \frac{dx}{1+x^b} + \text{constant} \tag{61}$$

If the integration on the right hand side of Equation 61 can be performed, an analytical solution can be obtained. However, because b is not restricted to integer values, it is quite difficult to perform the integration. For many values of b, a method has been found for performing the integration (see Appendix). The analytical solutions for these cases are,

$$y_o = (1+x^b)^{\frac{(-1)^{\frac{n+1}{2}} - b}{b}} \exp(-2/b) \sum_{j=1}^{\frac{n-1}{2}} (-1)^{j+1} \frac{(x^{b/2})^{n-(2j-1)}}{n-(2j-1)} \tag{62}$$

where $0 < b < 1$, $n \equiv \frac{2}{b} - 1$ (an odd integer),

and

$$y_o = \frac{1}{1+x^b} \exp\{-(2/b)[\sum_{k=1}^{\frac{m}{2}} (-1)^{k+1} \frac{(x^{b/2})^{m-(2k-1)}}{m-(2k-1)} + (-1)^{m/2} \arctan x^{b/2}]\} \tag{63}$$

where $0 < b < 1$, $0 \leq \arctan x^{b/2} < \pi/2$, $m \equiv \frac{2}{b} - 1$ (an even integer) ≥ 2.

The p^{th} moment about the distributions of Equations 62 and 63 is

$$I^p = \int_0^\infty x^p\ y_o(x)dx \tag{64}$$

When the integral of Equation 64 is tested for convergence by the method described on page 18, I^p is found to converge for all $p \geq 0$ if b in Equations

62 and 63 is restricted to the interval $0 < b < 1$.

Figure 3 shows the effect of b on the dimensionless population distributions generated by Model-I. For the interval $0 < b < 1$, this model offers an improvement over the M-S growth rate model since one can determine a finite upper bound on the nuclei density by considering a nucleus to be of zero size. Nevertheless, although this model is an improvement over the M-S growth rate model, it probably has too many serious weaknesses for it to have any general application.

First, in order for the model to be continuous and satisfy the convergence criterion, b is restricted to the interval $0 < b < 1$. Bennett (2) presents experimental data which can only be correlated with negative values of b. Since the growth rate exponent, b, is restricted to positive values less than one, the versatility of the model is limited.

Second, as the crystal size apporaches zero, the rate of change of the growth rate with respect to size increases without bound. If the apparent dependency of crystal growth rate on size results from the effect of size on settling velocity, it does not seem likely that the growth rate of small crystals in an agitated suspension would change rapidly with size.

A third weakness, and perhaps the most serious weakness of Model-I, may be readily seen from Figure 3. This figure shows that even very small values of the growth rate exponent generate population distributions which deviate greatly from the ΔL Law distribution ($b=0$) at all crystal sizes. Again, considering the dependency of growth rate on size to result from the effect of size on settling velocity, one would not expect the population distributions for small crystals to differ greatly from the distribution generated by McCabe's ΔL Law.

Figure 3. Steady state dimensionless population density distributions defined by Equations 62 and 63

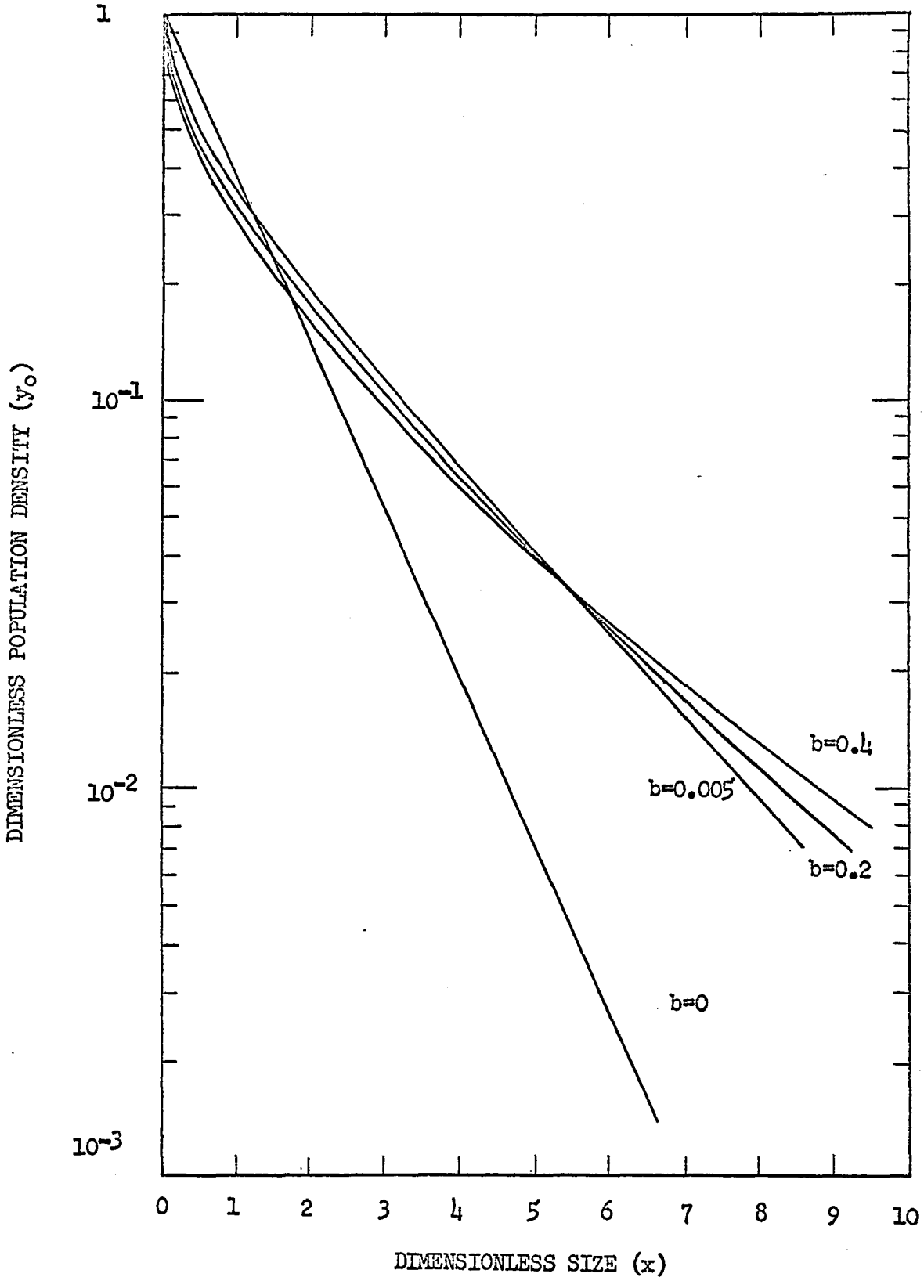
1
10^{-1}
10^{-2}
10^{-3}
DIMENSIONLESS POPULATION DENSITY (y_o)
0
1
2
3
4
5
6
7
8
9
10
DIMENSIONLESS SIZE (x)
b=0.4
b=0.005
b=0.2
b=0

Last, as the growth exponent decreases, the number of terms in the summations in Equations 62 and 63 increases rapidly, yielding complex expressions which are difficult to treat analytically.

Model-II

From an examination of the preceding two growth rate models and their steady state population density distributions, a number of desirable properties have been established for a realistic and useful growth rate expression. If the growth rate model can be put in the form,

$$r_o(L) = r_o^o \, f(L;b) \tag{65}$$

where $L \geq 0$, and $f(L;b)$ denotes a function involving the variable, L, and the exponent and parameter, b, these properties can be enumerated as:

1. The growth rate expression should be a continuous function of L and b in a region which includes the point (L=0, b=0).
2. The growth rate model should satisfy the condition, $r_o(0) \neq 0$.
3. The rate of change of the growth rate with respect to size should not increase or decrease without bound as the size approaches zero.
4. The zeroth moment and all positive moments of the population density distributions generated by the growth rate model should converge.
5. The population density distributions should not deviate greatly from the distribution predicted by McCabe's ΔL Law (b=0) for small crystal sizes.
6. The mathematical equations defining the distributions generated by the model should not be so complex as to make computational

techniques and costs prohibitive.

Neither of the preceding models satisfies all of the above points.

A growth rate model which has the from of Equation 65 and does satisfy all of the above points is

$$r_o(L) = r_o^o (1+\gamma L)^b \quad , \; b < 1 \qquad (66)$$

$$L \geq 0$$

From Equation 30, the steady state distributions corresponding to this model (Model-II) are

$$n_o(L) = K_3 \, n_o^o \, (1+\gamma L)^{-b} \exp\left[-\frac{(1+\gamma L)^{1-b}}{1-b}\right] \qquad (67)$$

where $K_3 = \exp\left(\frac{1}{1-b}\right)$ and $b < 1$.

Substituting the dimensionless variables defined by Equations 57 and 58 into Equation 67,

$$y_o(x) = K_3(1+x)^{-b} \exp\left[-\frac{(1+x)^{1-b}}{1-b}\right] \quad , \; b < 1 \qquad (68)$$

Again, using the technique described on page 18, the zeroth moment and all positive moments of the distributions defined by Equation 68 can be shown to converge. This satisfies the fourth condition listed on page 30. (The reason why b is once again found to be restricted to the same interval for convergence, $b < 1$, should be evident. As the size of a crystal increases without bound, Model-I and Model-II become identical to the M-S growth rate expression.)

Figure 4 is a plot of the dimensionless population distributions of Equation 68. By examining Figure 4 and Equations 66 and 68, it can be seen that Model-II satisfies the remaining conditions on page 30.

Figure 4. Steady state dimensionless population density distributions defined by Equation 68

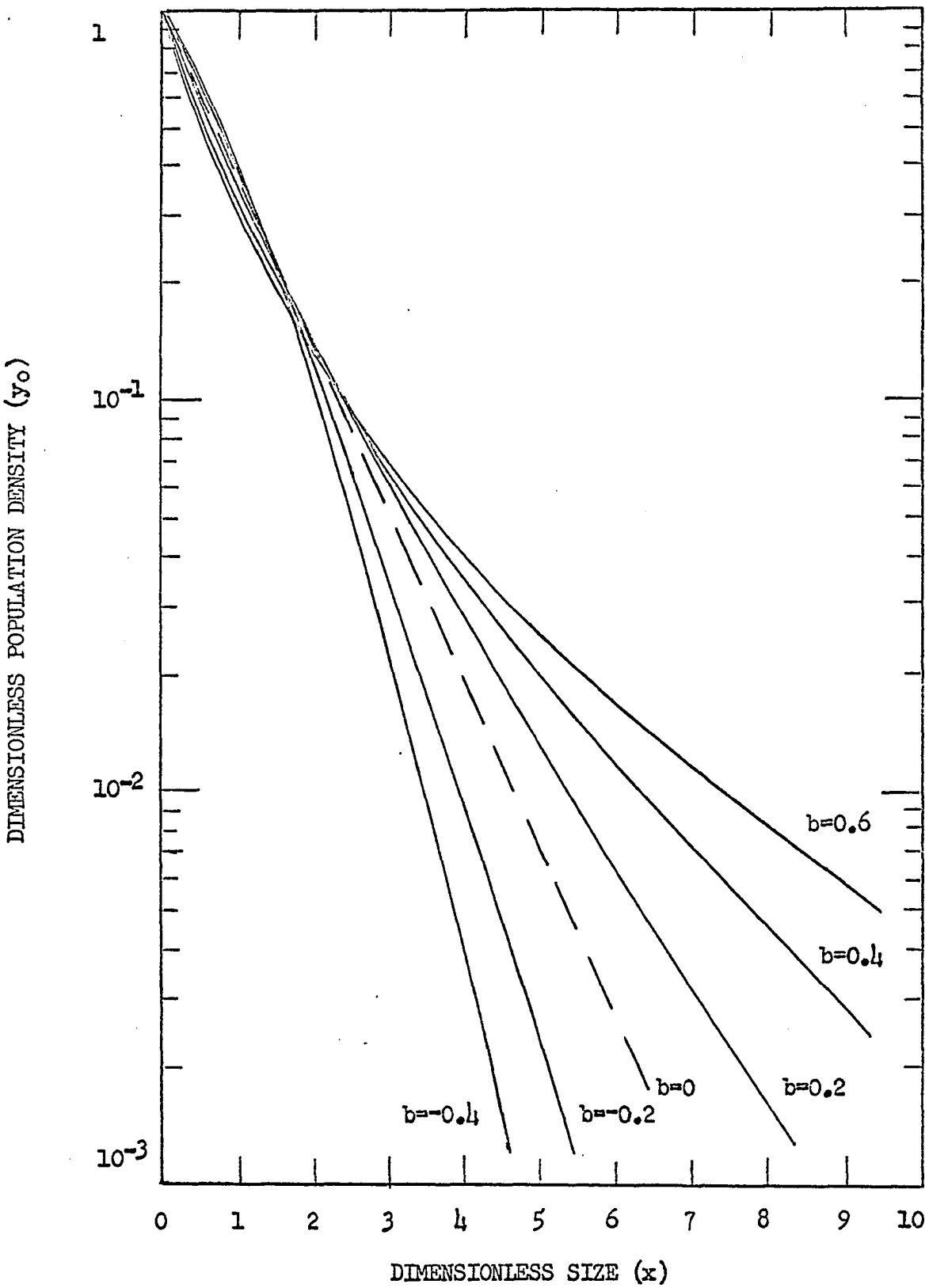
DIMENSIONLESS POPULATION DENSITY (y_o)
1
10^{-1}
10^{-2}
10^{-3}
0
1
2
3
4
5
6
7
8
9
10
DIMENSIONLESS SIZE (x)
b=0.6
b=0.4
b=0.2
b=0
b=-0.2
b=-0.4

Application to Experimental Data

For reasons already discussed, it is desirable, both from a practical and a theoretical standpoint, for a growth rate model to satisfy many or all of the conditions listed on page 30. However, in the final analysis, if a model satisfies these conditions but does not fit experimental data, it is of no practical use and may have only academic interest.

Unfortunately, it is extremely difficult to find data in the literature where the crystal growth occurred under conditions approximating those in an industrial CMSMPR crystallizer. The classical growth rate experiments involve the growth of single crystals or monosized crystals in a batch crystallizer, under conditions such that little or no nucleation occurs. In industrial crystallizers, both growth and nucleation take place simultaneously, and the energy, feed, and product streams are controlled to maintain constant temperature, supersaturation, and suspension density.

In investigating the theoretical model of Randolph and Larson (14), Chambliss (5) constructed a 10 1/2 liter cooling, CMSMPR, crystallizer. Growth and nucleation take place in this type of a crystallizer under conditions which more closely resemble those in an industrial crystallizer. In most of his experiments, Chambliss found that the crystal growth obeyed McCabe's ΔL Law. However, in a few of his early experiments, where the agitation was not as efficient or intense as in later experiments, Chambliss[1] collected steady state size distribution data which indicate a

---

[1]Chambliss, C. W. Ames, Iowa. Nucleation and growth in a cooling crystallizer. Private communication. 1966.

possible departure from the ΔL Law. Data which are representative of that obtained by Chambliss are shown in Figures 5 and 6. Figure 5 is a plot of a steady state size distribution for alum; Figure 6 is a similar plot for tartaric acid.

From these figures it is seen that the distributions of the larger crystals depart from the distribution predicted by McCabe's ΔL Law (b=0). At the larger crystal sizes, the number of crystals present exceed that predicted by the ΔL Law.

It is important to recognize, however, that one cannot conclude from these data that the distributions are the result of a size dependent crystal growth rate. Classification and accumulation of the larger crystals, or crystal agglomeration, could also have produced the same result. (Chambliss[1] conducted experiments which seem to indicate that the alum distribution is the result of imperfect mixing, and localized classification and accumulation of the larger size crystals.) In any case, the data do show a departure from the ΔL Law distribution, and can be analyzed on the basis of a size dependent crystal growth rate.

If the ΔL Law holds, and growth rate is independent of crystal size, Equation 30 can be solved for the steady state size distribution,

$$n_o(L) = n_o^o \exp(-L/r_o T_o) \tag{69}$$

This distribution, which was originally derived by Bransom et al. (4a), can also be obtained by letting b=0 in Equation 67 if γ is defined as, $\gamma = 1/r_o^o T_o$.

---

[1] Ibid.

Figure 5. Steady state size distribution data obtained by Chambliss for alum. T_o = 30 min. $n_o^o = 6.6 \times 10^6$, r_o^o = 0.00204 m.m./min.

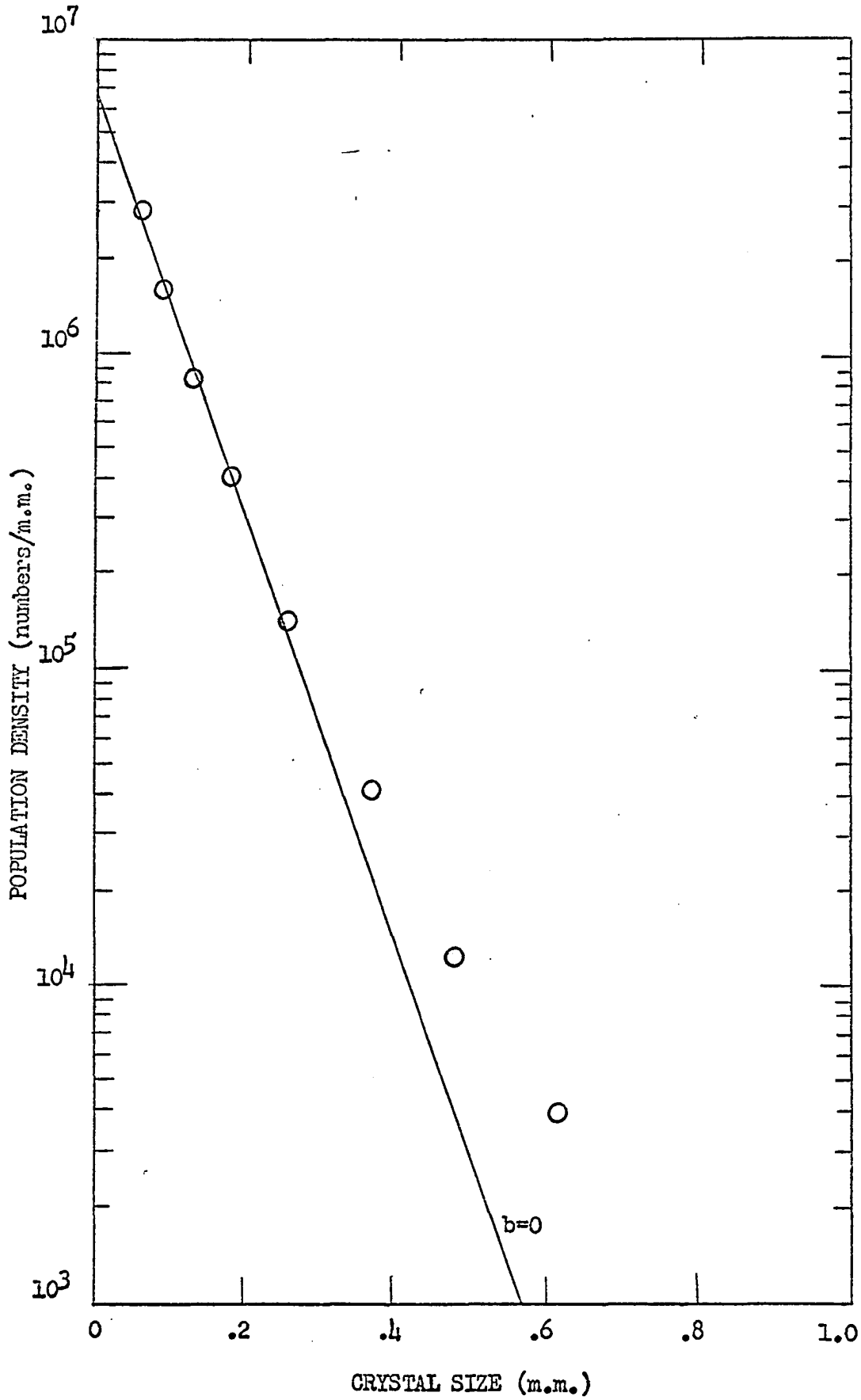
10^7
10^6
10^5
10^4
10^3
POPULATION DENSITY (numbers/m.m.)
b=0
0
.2
.4
.6
.8
1.0
CRYSTAL SIZE (m.m.)

Figure 6. Steady state size distribution data obtained by Chambliss for tartaric acid. T_o = 45 min. $n_o^o = 3.0 \times 10^6$, r_o^o = 0.00069 m.m./min.

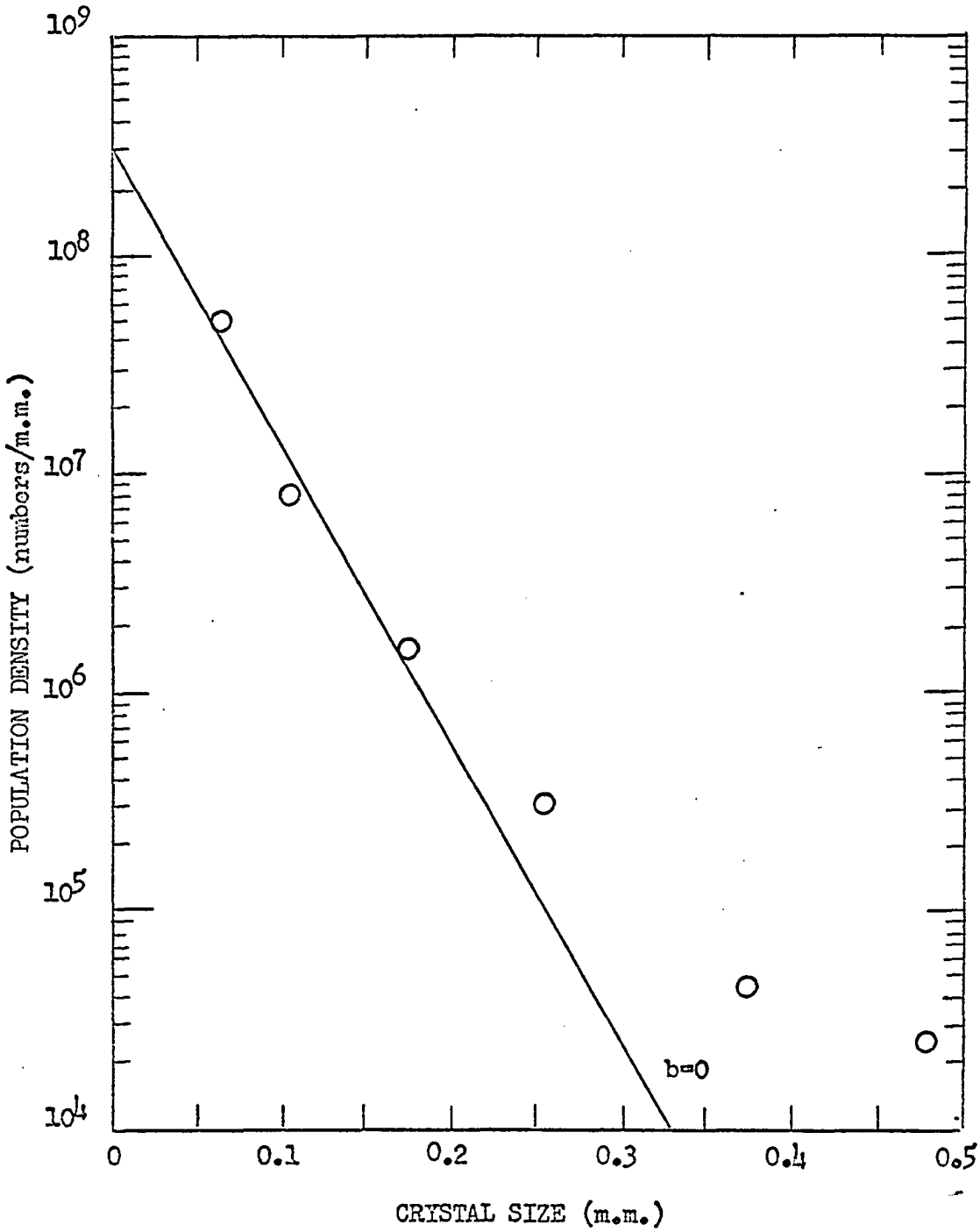
POPULATION DENSITY (numbers/m.m.)
10^9
10^8
10^7
10^6
10^5
10^4
b=0
0
0.1
0.2
0.3
0.4
0.5
CRYSTAL SIZE (m.m.)

Taking the logarithm of both sides of Equation 69

$$\ell n\ n_o(L) = \ell n\ n_o^o - L/r_o T_o \tag{70}$$

From Equation 70 it is seen that a plot of the logarithm of the population density versus crystal size should result in a straight line with a slope equal to $-1/r_o T_o$, and an intercept equal to the logarithm of the nuclei density.

In an agitated suspension where crystal growth rate is a function of crystal size, it seems reasonable to expect that only the larger crystals would have a relative crystal-solution velocity significantly different than the bulk velocity of the liquid phase. If the apparent effect of size on crystal growth rate results from the effect of size on settling velocity, one would expect small crystals to grow at an approximately constant rate. Therefore, the distribution of small crystals should not depart greatly from that predicted by McCabe's ΔL Law, Equation 69.

Figure 4 on page 33 is a plot of some dimensionless population density distributions generated by the Model-II growth rate expression, $r_o = r_o^o(1+\gamma L)^b$. From Figure 4 it can be seen that the straight line ΔL Law distribution (b=0) gives a good approximation of the distribution of small crystals for other values of b. Thus, assuming that the small crystals grow at a nearly constant rate, r_o^o, Equation 70 can be used to determine r_o^o and n_o^o from experimental data, if a plot of the logarithm of the population density versus crystal size results in the small crystals being approximately linearly distributed.

From Figures 5 and 6 it is seen that the small crystals are approximately linearly distributed. From the linear portions of these curves,

r_o^o and n_o^o have been determined for the respective distributions. Using the dimensionless variables defined by Equations 57 and 58, the data in Figures 5 and 6 have been replotted in dimensionless form in Figures 7 and 8.

Both the alum and tartaric acid data, Figures 7 and 8 respectively, can be fit reasonably well with the steady state distribution generated by Model-II for b=0.2 (Equation 68). In both cases, however, the population density of the largest analyzed crystal size exceeds the predicted value. If the data exhibit a true size dependent growth rate, this could be the result of agglomeration or a weakness of the growth rate model.

A discussion of errors involved in determining r_o^o, n_o^o, and b from experimental data by the technique described is warranted. First, it is assumed that the population density distribution of the small crystals can be approximated by a straight line ΔL Law distribution (b=0). Because there is always some scattering of the data, it is not always obvious how many of the data points should be regarded as falling on a straight line. Second, once it has been decided which data points are to be regarded as falling on a straight line, it is often not apparent how the straight line should be drawn through the data points. Because it is more difficult to accurately determine the distribution of crystals which have a size less than 100 microns, data points corresponding to sizes less than 100 microns may be more in error than data points corresponding to larger crystal sizes. Since the population density is plotted on a logarithmic scale, small changes in the slope of the line, $-\frac{1}{r_o^o T_o}$,

Figure 7. Dimensionless plot of the size distribution data in Figure 5

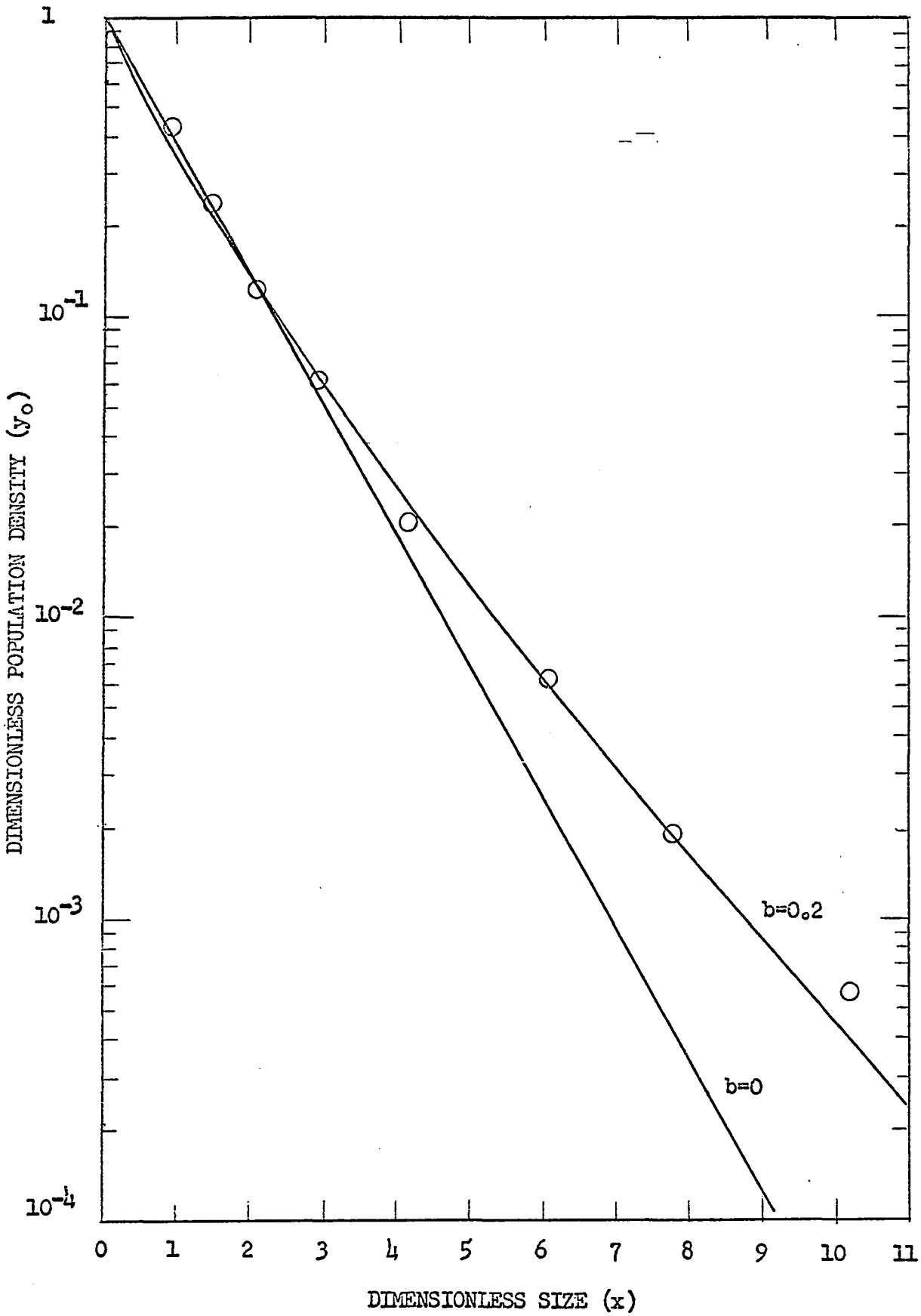
1
10^{-1}
10^{-2}
10^{-3}
10^{-4}
DIMENSIONLESS POPULATION DENSITY (y_o)
0
1
2
3
4
5
6
7
8
9
10
11
DIMENSIONLESS SIZE (x)
b=0.2
b=0

Figure 8. Dimensionless plot of the size distribution data in Figure 6

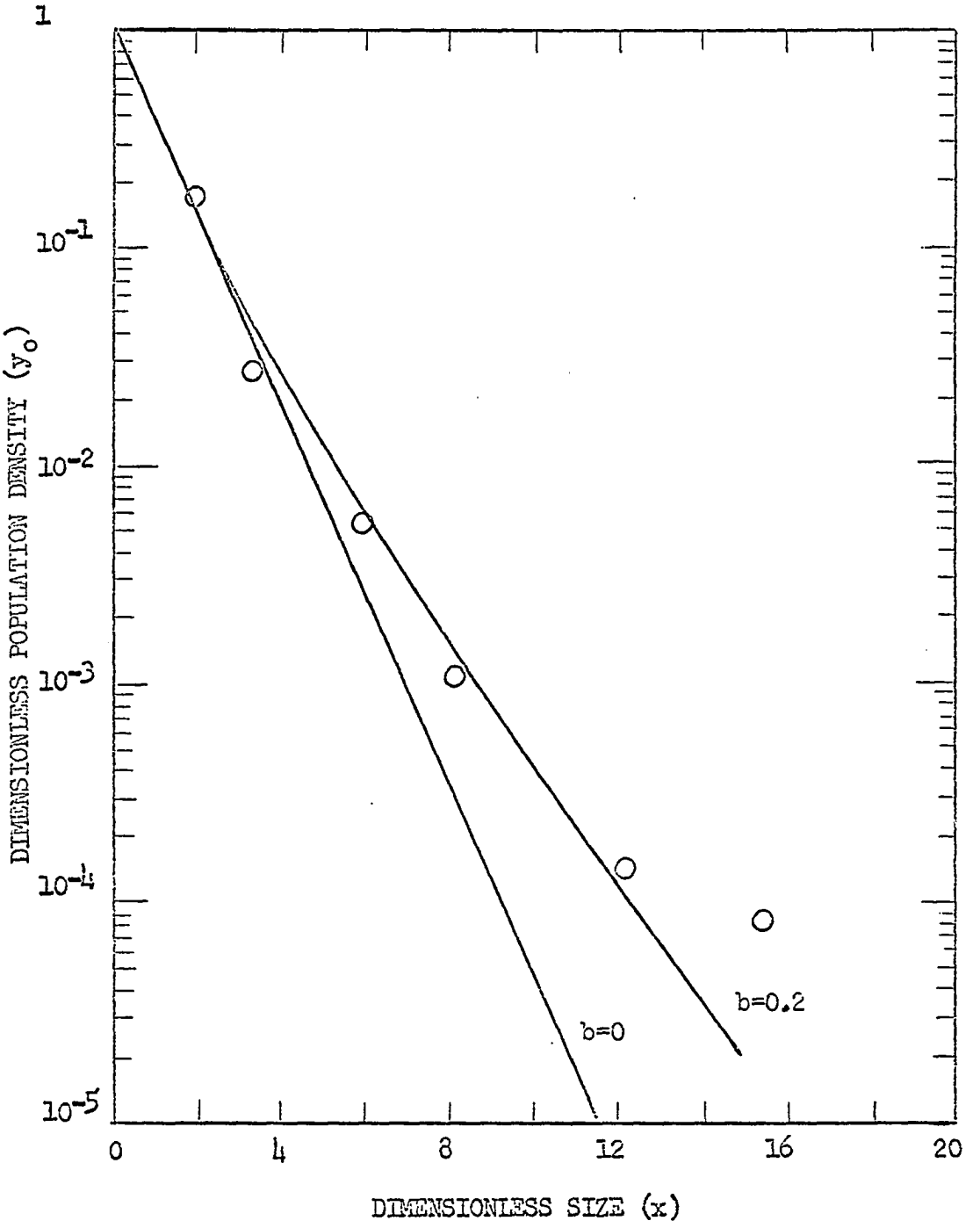
1
10^{-1}
10^{-2}
10^{-3}
10^{-4}
10^{-5}
DIMENSIONLESS POPULATION DENSITY (y_o)
0
4
8
12
16
20
DIMENSIONLESS SIZE (x)
b=0.2
b=0

can make a significant difference in the intercept, n_o^o, and effect the value of the parameter, b.

For example, consider the alum data in Figure 5. Values of $r_o^o T_o$ = 0.067 m.m. and $n_o^o = 6.0 \times 10^6$ numbers/m.m. give b = 0.15; $r_o^o T_o$ = 0.061 m.m. and $n_o^o = 6.6 \times 10^6$ numbers/m.m. give b = 0.20; $r_o^o T_o$ = 0.056 m.m. and $n_o^o = 8.0 \times 10^6$ numbers/m.m. give b = 0.25. As is often the case when using experimental data, a knowledge of the procedures and analytical methods employed in obtaining the data can be very important in deciding how the data is to be treated.

In a recent paper by Canning and Randolph (4b), population density distribution data are presented which show a departure from the ΔL Law distribution. These data, which were obtained from a bench scale CMSMPR crystallizer for Glauber's salt, are shown in Figure 9. The authors realized that the departure from the ΔL Law distribution could be due to classification, agglomeration, particle breakage, seed dissolving, crystals not remaining geometrically similar during growth, nonsteady state operation, or a size dependent growth rate. However, based on their study of the system, the authors have ruled out all of the above causes except the latter, and they believe the departure from the ΔL Law distribution is due to a size dependent growth rate.

Using the technique described on page 40 to determine $r_o^o T_o$ and n_o^o, and the dimensionless variables defined by Equations 57 and 58, the Glauber salt data of Figure 9 were replotted in dimensionless form in Figure 10. A trial and error procedure was then used to determine which of the dimensionless steady state distributions generated by the Model-II

Figure 9. Steady state size distribution data obtained by Canning and Randolph (4b) for Glauber's salt. The values of n_o^o and $r_o^o T_o$ for the Model-II growth rate expression are: $n_o^o = 8.0 \times 10^6$, $r_o^o T_o = 0.08$ m.m.

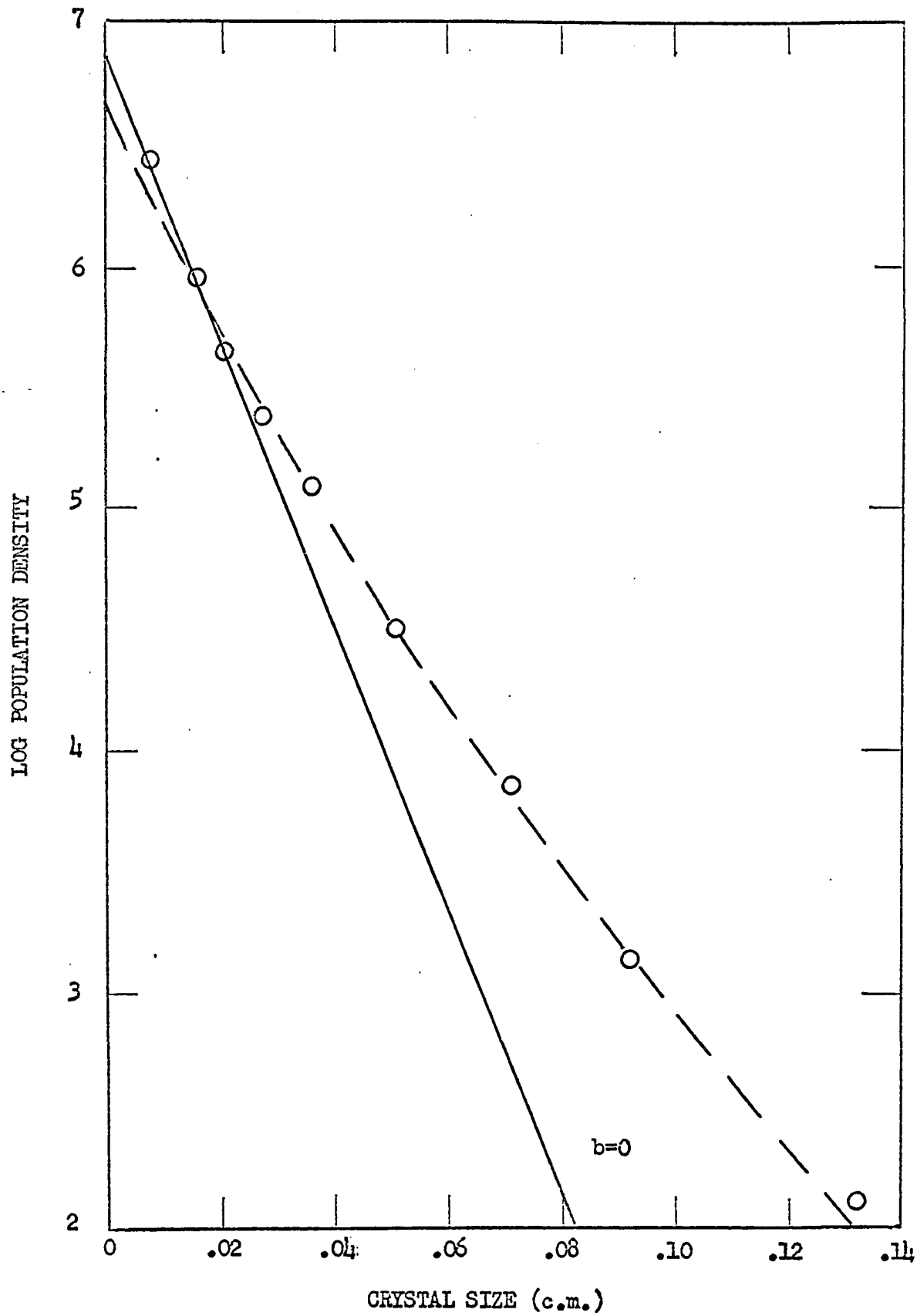
7
6
5
4
3
2
LOG POPULATION DENSITY
0
.02
.04
.06
.08
.10
.12
.14
CRYSTAL SIZE (c.m.)
b=0

Figure 10. Dimensionless plot of the size distribution data in Figure 9

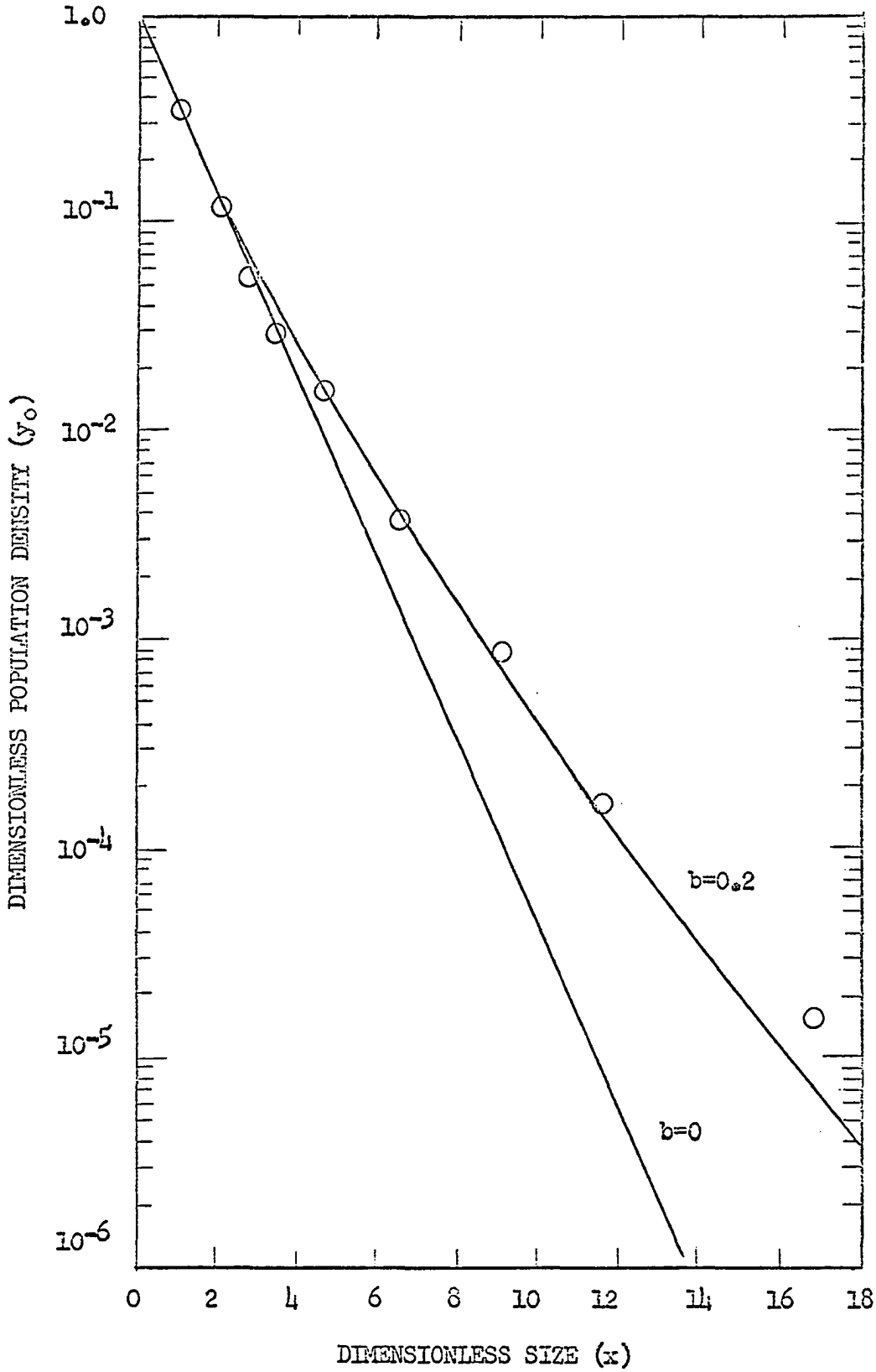
1.0
10^{-1}
10^{-2}
10^{-3}
10^{-4}
10^{-5}
10^{-6}
DIMENSIONLESS POPULATION DENSITY (y_o)
0
2
4
6
8
10
12
14
16
18
DIMENSIONLESS SIZE (x)
b=0.2
b=0

growth rate expression would provide the best fit of the data. Again, the distribution for b=0.2 was found to give the best results. The fit provided by this distribution is shown in Figure 10.

Canning and Randolph (4b) propose the equation

$$r_o = r_o^o (1 + \gamma L) \tag{71}$$

to describe the relationship between size and growth rate. This is simply the Model-I or Model-II growth rate expression with b=1. The distributions generated by this growth rate expression are

$$n_o = n_o^o (1 + \gamma L)^{-(\frac{J+1}{J})} \tag{72}$$

where $J = \gamma r_o^o T_o$. For the Glauber salt data, Canning and Randolph found that a value of J = 0.065 provided the best fit. This is shown as the dashed line in Figure 9. From Figure 9, it is seen that their model does indeed provide a good fit of the data.

However, when moments of the distributions are tested for convergence, a weakness of the growth rate model proposed by Canning and Randolph is discovered. The $p^{\underline{th}}$ moment about the distribution of Equation 72 is

$$I^p = \int_o^\infty L^p n_o \, dL \tag{73}$$

In order for the above integral to converge, p is restricted to the interval

$$p < \frac{1}{J} \tag{74}$$

Since the zeroth moment and positive moments of the distributions can be assigned physical meaning, this restriction should not exist.

From Figures 9 and 10, it is seen that the Model-II distribution for

b=0.2 gives a fit of the data comparable to that provided by the distribution of Canning and Randolph (4b). The Model-II growth rate expression has the added advantage, however, that the zeroth moment and all positive moments of the distributions generated by it are found to converge. Also, the Model-II growth rate expression has the capability of fitting data which exhibit a growth rate inversely proportional to crystal size; this is not possible with the model of Canning and Randolph.

TRANSIENT SIZE DISTRIBUTION BEHAVIOR

Derivation of Equations

If a CMSMPR crystallizer is operated so that no particles are present in the input stream(s) and a constant suspension volume is maintained, Equation 23 reduces to

$$\frac{\partial n}{\partial t} + \frac{\partial}{\partial L}(rn) + \frac{n}{T} = 0 \tag{75}$$

where the growth rate, r, can be a function of the crystal size. Equation 75 predicts the transient behavior of the crystal population density. At steady state, the Model-II growth rate expression is

$$r_o = r_o^o (1 + \gamma L)^b \quad , b < 1 \tag{76}$$

Since the growth rate is a function of the supersaturation, from experimental evidence (6,9) it seems reasonable to assume that

$$r_o^o = k\, s_o^a \quad , a \geq 1 \tag{77}$$

Thus, the unsteady state Model-II growth rate expression can be written as

$$r = k\, s^a (1 + \gamma L)^b, \quad \begin{matrix} a \geq 1 \\ b < 1 \end{matrix} \tag{78}$$

Substituting Equation 78 into Equation 75

$$\frac{\partial n}{\partial t} + k\, s^a (1 + \gamma L)^b \frac{\partial n}{\partial L} + \gamma b\, k\, s^a (1 + \gamma L) n^{b-1} + \frac{n}{T} = 0 \tag{79}$$

During unsteady state operation, the supersaturation, s, is not constant but varies with time. Hence, Equation 79 has two dependent variables, n and s. In order to solve Equation 79 for transient crystal population density behavior, an independent equation is needed which describes supersaturation as a function of time.

The total crystal mass in the suspension is

$$M = \rho_s V \tag{80}$$

where ρ_s is the suspension density and V is the suspension volume. The total crystal mass can also be written as

$$M = \rho_s k_v \int_0^\infty n L^3 dL \tag{81}$$

If the crystallizer is operated so that a constant suspension density and a constant suspension volume are maintained, the total crystal mass is constant, and

$$\frac{dM}{dt} = \frac{d}{dt}\{\rho_c k_v \int_0^\infty n L^3 dL\} = 0 \tag{82}$$

or

$$\int_0^\infty \frac{\partial n}{\partial t} L^3 dL = 0 \tag{83}$$

Substituting the expression for $\frac{\partial n}{\partial t}$ from Equation 79 into Equation 83 gives

$$k s^a \int_0^\infty (1 + \gamma L)^b L^3 \frac{\partial n}{\partial t} dL + \gamma b k s^a \int_0^\infty n(1 + \gamma L)^{b-1} L^3 dL$$

$$+ \frac{1}{T} \int_0^\infty n L^3 dL = 0 \tag{84}$$

Integrating the first integral on the left hand side of Equation 84 by parts

$$\int_0^\infty (1 + \gamma L)^b L^3 \frac{\partial n}{\partial L} dL = (1 + \gamma L)^b L^3 n \Big|_0^\infty$$

$$- \gamma b \int_0^\infty n(1 + \gamma L)^{b-1} L^3 dL - 3 \int_0^\infty n(1 + \gamma L)^b L^2 dL \tag{85}$$

Since moments about the distribution must converge

$$(1 + \gamma L)^b L^3 \, n \, \Big|_0^\infty = 0 \tag{86}$$

and

$$\int_0^\infty (1 + \gamma L)^b L^3 \frac{\partial n}{\partial L} \, dL = - \gamma b \int_0^\infty n(1 + \gamma L)^{b-1} L^3 \, dL$$

$$- 3 \int_0^\infty n(1 + \gamma L)^b L^2 \, dL \tag{87}$$

Substituting the expression for the integral on the left hand side of Equation 87 into Equation 84 and rearranging

$$k \, s^a = \frac{\int_0^\infty n \, L^3 \, dL}{3T \int_0^\infty n(1 + \gamma L)^b L^2 \, dL} \tag{88}$$

Since the total crystal mass is assumed to remain constant, Equation 88 can be written as

$$k \, s^a = \frac{\int_0^\infty n_o \, L^3 \, dL}{3T \int_0^\infty n(1 + \gamma L)^b L^2 \, dL} \tag{89}$$

Equations 79 and 89 form a set of two independent equations which, with the appropriate initial and boundary conditions, can be solved simultaneously to give the transient response of the crystal population density to various changes in crystallizer operating conditions.

If the crystallizer is operating at steady state prior to a change in operating conditions, the initial condition is simply the steady state distribution, or

$$n_o = n(L,t=0) = K_3\, n_o^o\, (1 + \gamma L)^{-b} \exp[-\frac{(1 + \gamma L)^{1-b}}{1-b}] \qquad (90)$$

where $K_3 = \exp(\frac{1}{1-b})$ and $b < 1$. The boundary condition can be derived by considering the rate of formation of nuclei.

At steady state, the nucleation rate is

$$\frac{dN_o^o}{dt} = (\frac{dN}{dL})_{\substack{L=0 \\ s.s.}} \cdot (\frac{dL}{dt})_{\substack{L=0 \\ s.s.}} = n_o^o\, r_o^o \qquad (91)$$

where "s.s." refers to steady state conditions. Expressing the nucleation rate in terms of the supersaturation

$$\frac{dN_o^o}{dt} = k_N\, s_o^\alpha \qquad (92)$$

Equating the right hand sides of Equations 91 and 92

$$n_o^o\, r_o^o = k_N\, s_o^\alpha \qquad (93)$$

For the transient state, Equation 93 can be written as

$$n^o\, r^o = k_N\, s^\alpha \qquad (94)$$

Combining Equations 93 and 94

$$\frac{n^o\, r^o}{n_o^o\, r_o^o} = (\frac{s}{s_o})^\alpha \qquad (95)$$

From Equation 77, r^o can be expressed as

$$r^o = k\, s^a \quad , \quad a \geq 1 \qquad (96)$$

Substituting Equation 77 and 96 into Equation 95, and solving for n^o

$$n^o = n_o^o\, (\frac{s}{s_o})^{\alpha-a} \qquad (97)$$

Equation 97 is the required boundary condition. It shows how the nuclei

density is related to the steady state nuclei density, the supersaturation, and the nucleation and growth rate exponents α and a.

It is interesting to note that whenever α=a, the nuclei density remains constant, and hence, disturbances in the system do not change the crystal size distribution. Timm (17) observed this when he numerically solved the transient population density distribution equation assuming that McCabe's ΔL Law held and α=a=1.

Solving for s from Equation 89, Equation 97 can also be written as

$$n^o = n(L=0,t) = n_o^o \left[\frac{\frac{T_o}{T}\int_o^\infty n_o(1+\gamma L)^b L^2\, dL}{\int_o^\infty n(1+\gamma L)^b L^2\, dL}\right]^{\frac{\alpha-a}{a}} \tag{98}$$

Comparing Equation 98 with Equations 96 and 97, it can be seen that

$$\frac{r^o}{r_o^o} = \left[\frac{\frac{T_o}{T}\int_o^\infty n_o(1+\gamma L)^b L^2\, dL}{\int_o^\infty n(1+\gamma L)^b L^2\, dL}\right] \tag{99}$$

The value of the constant, $\frac{\alpha-a}{a}$, in Equation 98 can be determined from experimental data. From Equation 77,

$$s_o = \left(\frac{r_o^o}{k}\right)^{\frac{1}{a}} \tag{100}$$

Substituting the expression for s_o from Equation 100 into Equation 93

$$k_N \left(\frac{r_o^o}{k}\right)^{\frac{\alpha}{a}} = n_o^o\, r_o^o \tag{101}$$

or

$$K_N (r_o^o)^{\frac{\alpha-a}{a}} = n_o^o \tag{102}$$

Taking the logarithm of both sides of Equation 102

$$\ell n\ n_o^o = \ell n\ K_N + \left(\frac{\alpha-a}{a}\right) \ell n\ r_o^o \tag{103}$$

From Equation 103 it is seen that, if a number of steady state experimental runs are made and n_o^o and r_o^o are determined for each run, a plot of the logarithm of n_o^o versus the logaithm of r_o^o will yield a straight line having a slope equal to $(\frac{\alpha-a}{a})$. This procedure has been used to determine this constant for a number of crystalline materials (5,10,13, 18).

If the expression for $k\ s^a$ from Equation 89 is substituted into Equation 79, and the dimensionless variables

$$y = \frac{n}{n_o^o} \tag{104}$$

$$x = \gamma L = \frac{L}{r_o^o\ T_o} \tag{105}$$

$$\theta = \frac{t}{T_o} \tag{106}$$

are introduced, Equations 79, 90, 98, and 99 can be written in dimensionless form as

$$\frac{\partial y}{\partial \theta} + \frac{T_o}{T}\,\phi(1+x)^b\,\frac{\partial y}{\partial x} + b\,\frac{T_o}{T}\,\phi(1+x)^{b-1}\,y + \frac{T_o}{T}\,y = 0 \tag{107}$$

$$y_o = y(x,0) = K_3(1+x)^{-b}\,\exp\left[-\frac{(1+x)^{1-b}}{1-b}\right] \tag{108}$$

$$y^o = y(0,\theta) = \left[\frac{\frac{T_o}{T}\int_o^\infty y_o\,(1+x)^b\,x^2\,dx}{\int_o^\infty y\,(1+x)^b\,x^2\,dx}\right]^{\frac{\beta}{a}} = \left(\frac{r_o^o}{r_o}\right)^{\frac{\beta}{a}} \tag{109}$$

where

$$\phi = \frac{\int_0^\infty y_o\, x^3\, dx}{3\int_0^\infty y(1+x)^b x^2\, dx} \tag{110}$$

and

$$\beta = \alpha - a \tag{111}$$

Equation 107, together with the initial and boundary conditions, Equations 108 and 109, can be solved to give the transient response of the dimensionless population density distribution to various change in crystallizer operating conditions. Equations 107 through 109 were solved on an IBM 360 Model 50 digital computer using finite difference techniques for a step change in crystallizer production rate at different values of the growth rate parameter, b. The equations were also solved for a step change in b, keeping the production rate constant. Only first order finite differences were used.

Equation 107 in differenced form is

$$y_J^{I+1} = -\frac{T_o}{T}\phi[1+x_J]^b \frac{\Delta\theta}{2\Delta x}[y_{J+1}^I - y_{J-1}^I] + [1 - b\frac{T_o}{T}(1+x_J)^{b-1}\Delta\theta - \frac{T_o}{T}\Delta\theta]\, y_J^I \tag{112}$$

where the index, J, refers to positions in the x-direction of the grid and the index, I, refers to positions in the θ-direction of the grid. In order to have a stable solution it was found that a value of $\Delta\theta \leq 0.0025$ was required. A value of $\Delta x = 0.05$ was used to approximate the derivative in the x-direction. The computer program which was used for the numerical solution can be found in the Appendix.

As $b \to 1$, the values of the integrals in Equations 109 and 110 increase without bound. Figure 11 is a plot of the steady state dimensionless mass distribution function - i.e., the integrand of the integral in the numerator of Equation 110. From Figure 11 it can be seen that as b is increased, wider ranges of integration are required in order for the numerical integration to give a good approximation of the actual value of the integral. Of course, as the range of numerical integration increases, so does the amount of computer time required, and hence, the computational cost.

Step Change in Production Rate

Assuming that McCabe's ΔL Law was valid (b=0), and the nucleation and growth kinetics were fourth and first order respectively with regard to the supersaturation, Randolph and Larson (14) numerically solved the dimensionless transient population density equation for a step increase in production rate, $T_o/T = 1.25$. In order to investigate the effect of the Model-II growth rate expression on the transient response of the population density distribution, Equations 107 through 109 were solved for a step change in production rate, $T_o/T = 1.25$, for different values of the growth rate parameter, b. In each case it was assumed that the nucleation and growth kinetics were fourth and first order respectively with regard to the supersaturation - i.e., $\alpha=4$, $a=1$.

The transient responses for the different growth rates are shown in Figures 12 through 15. From examination of these figures, it can be seen that in each case the step increase in production rate causes a shower of nuclei to occur. As time passes, the nuclei which were members of this

Figure 11. A plot of the steady state mass distribution function for different values of the Model-II growth rate parameter, b

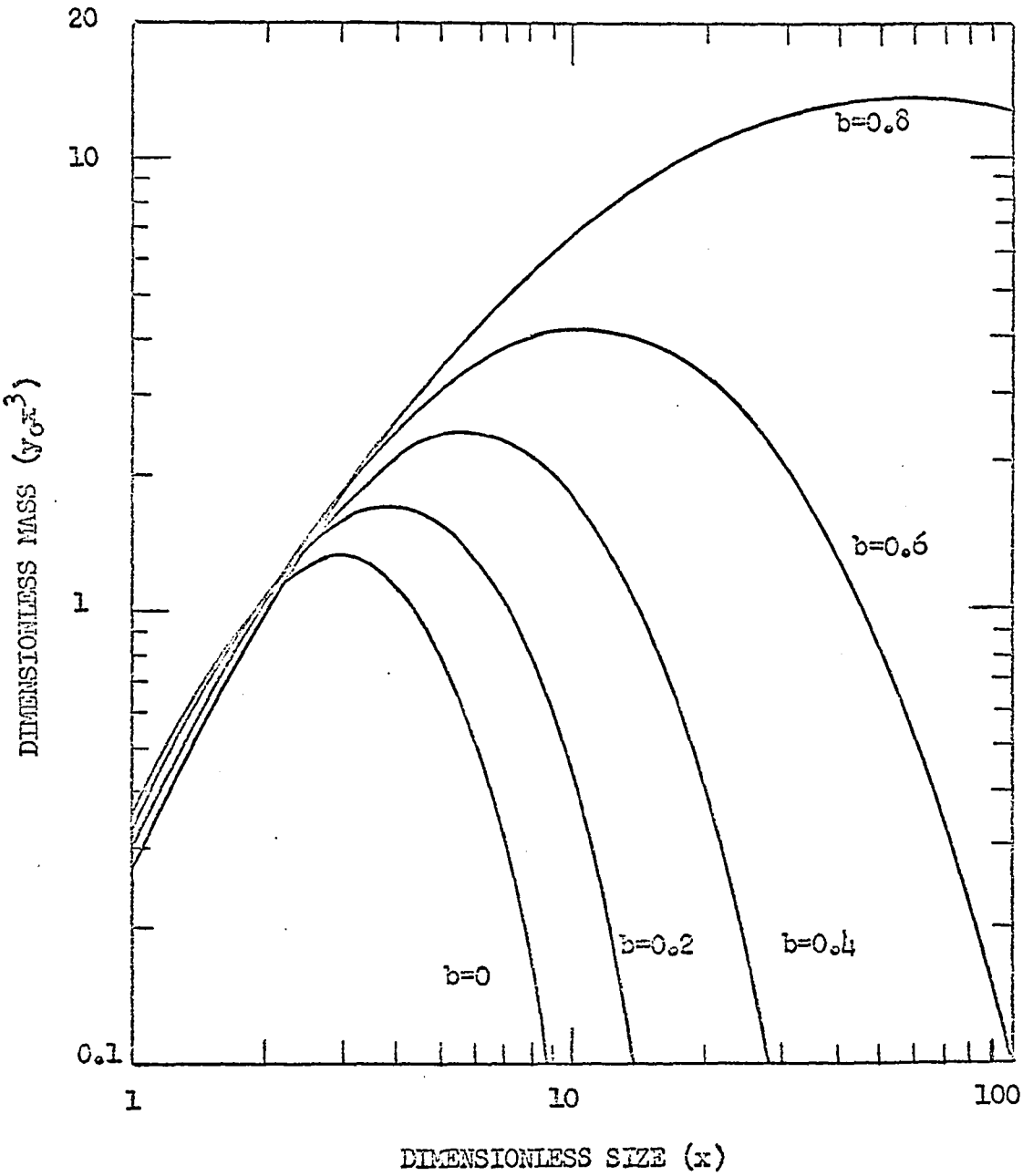
20
10
1
0.1
1
10
100
DIMENSIONLESS MASS ($y_0 x^3$)
DIMENSIONLESS SIZE (x)
b=0.8
b=0.6
b=0.4
b=0.2
b=0

Figure 12. Dimensionless plot of population density versus time for a step increase in production rate, $T_o/T = 1.25$, and $b = -0.2$

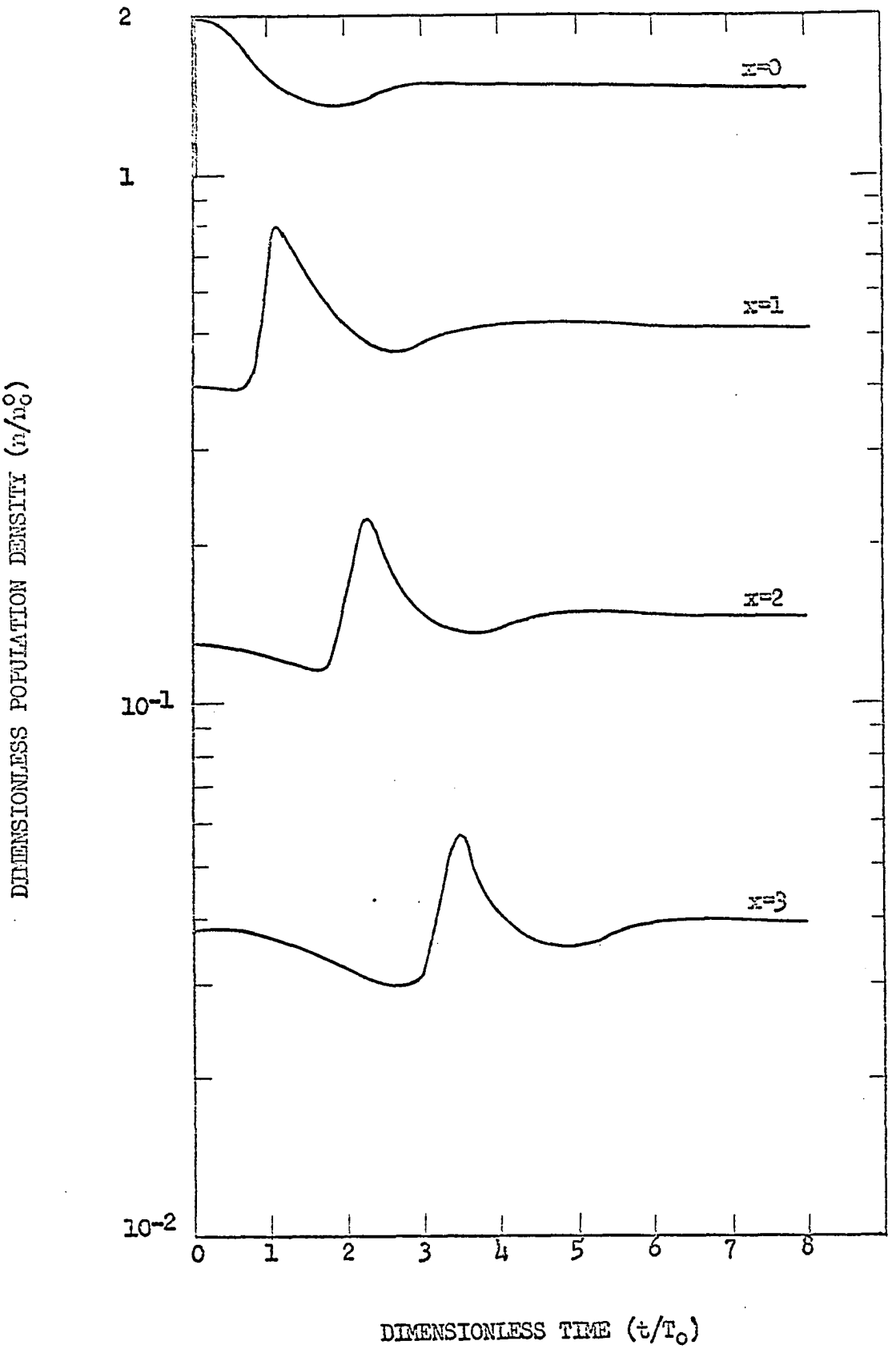
2
1
10-1
10-2
x=0
x=1
x=2
x=3
0
1
2
3
4
5
6
7
8
DIMENSIONLESS POPULATION DENSITY (n/n_0^0)
DIMENSIONLESS TIME (t/T_0)

Figure 13. Dimensionless plot of population density versus time for a step increase in production rate, $T_o/T = 1.25$, and $b = 0$

This was originally determined by Randolph and Larson (14)

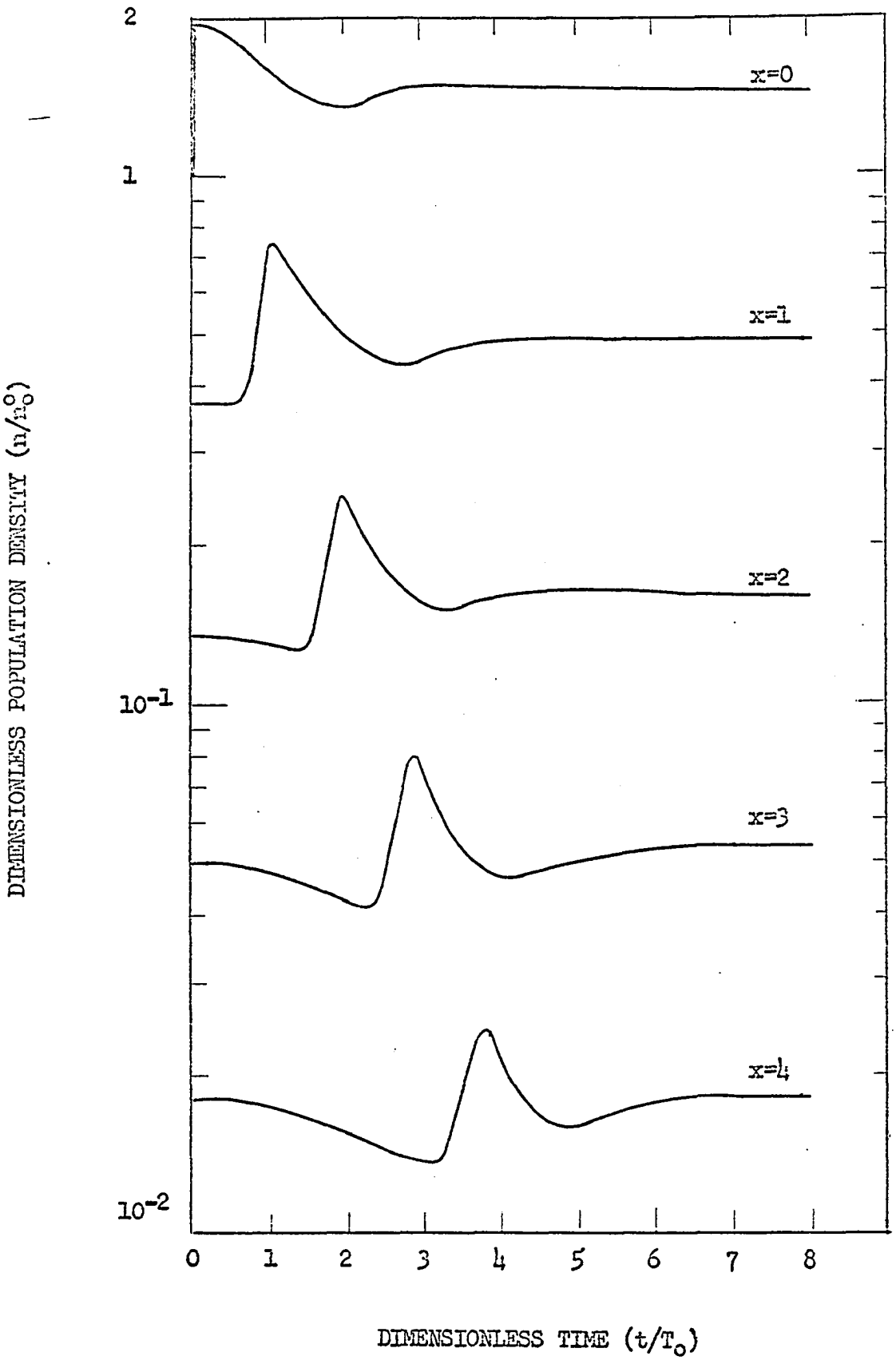
2
1
10^{-1}
10^{-2}
x=0
x=1
x=2
x=3
x=4
0
1
2
3
4
5
6
7
8
DIMENSIONLESS POPULATION DENSITY (n/n_o^0)
DIMENSIONLESS TIME (t/T_o)

Figure 14. Dimensionless plot of population density versus time for a step increase in production rate, $T_o/T = 1.25$, and $b = 0.2$

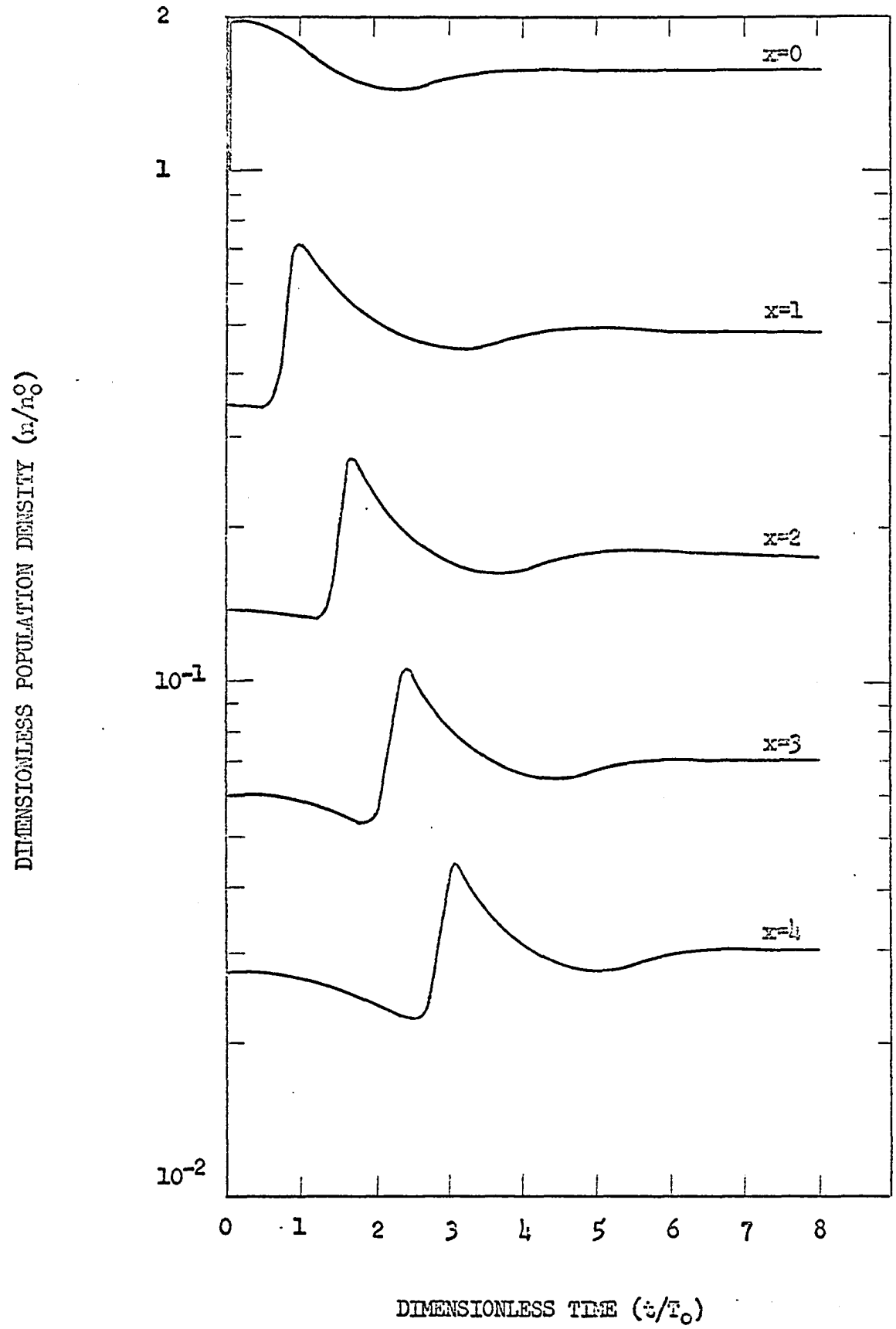
2
1
10^{-1}
10^{-2}
x=0
x=1
x=2
x=3
x=4
0
1
2
3
4
5
6
7
8
DIMENSIONLESS POPULATION DENSITY (n/n_o^0)
DIMENSIONLESS TIME (t/T_o)

Figure 15. Dimensionless plot of population density versus time for a step increase in production rate, $T_o/T = 1.25$, and $b = 0.4$

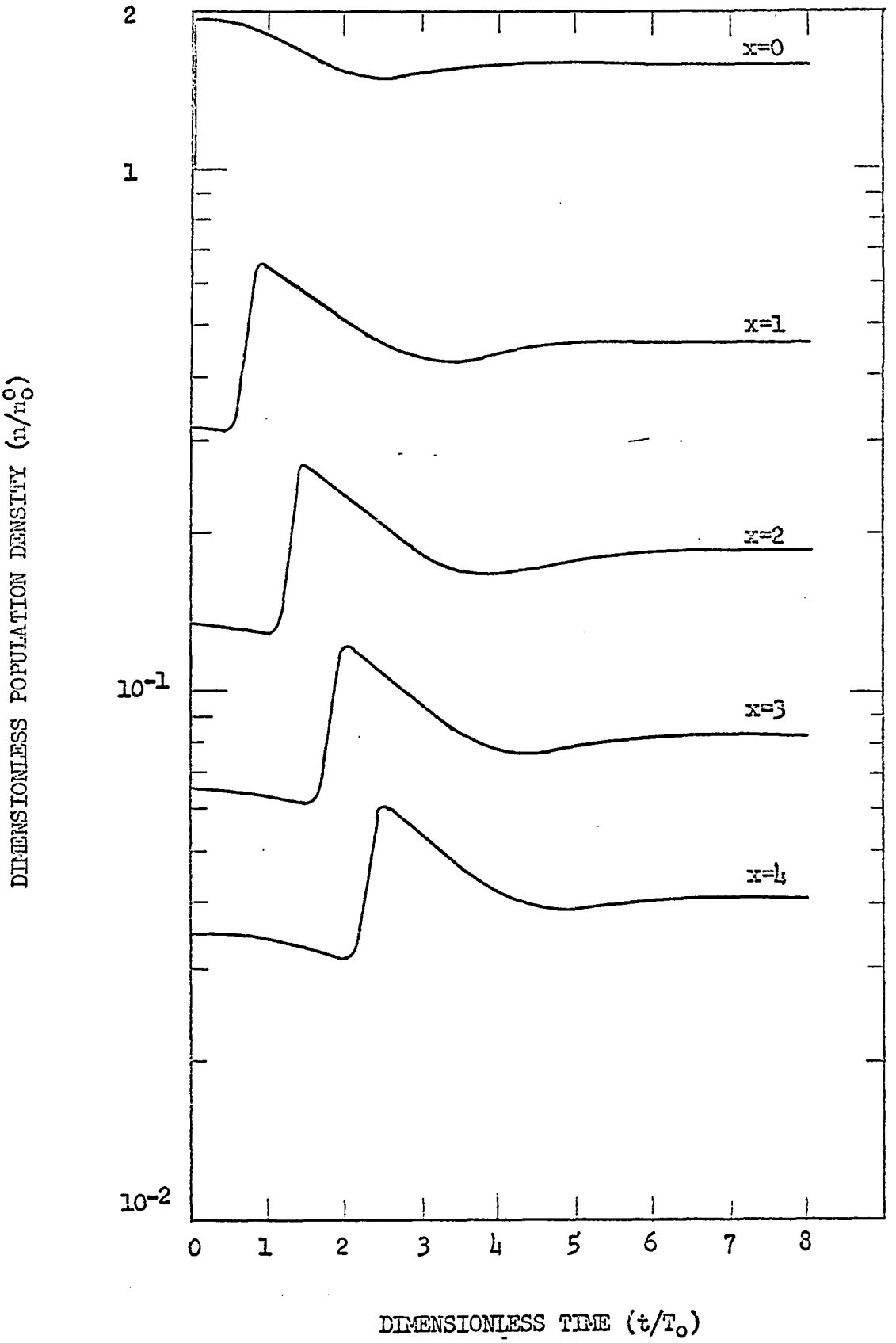
2
1
10^{-1}
10^{-2}
x=0
x=1
x=2
x=3
x=4
0
1
2
3
4
5
6
7
8
DIMENSIONLESS POPULATION DENSITY (n/n_o^0)
DIMENSIONLESS TIME (t/T_o)

shower grow into larger crystals, thereby causing transients in the population densities of all crystal sizes.

Figure 13 shows the transient behavior determined by Randolph and Larson (14) when it was assumed that McCabe's ΔL Law held (b=0). Comparing the transient responses for the size dependent growth rates, Figures 12, 14, 15, with the response obtained by Randolph and Larson Figure 13, it can be seen that the size dependent growth rates had no affect on the general behavior of the population density distribution to a step increase in production rate. The size dependent growth rates simply caused the disturbance in the nuclei density to grow through the crystal sizes at a faster or slower rate, depending on whether the crystal growth rate increased or decreased with size, that is, depending on whether b was greater or less than zero.

Irrespective of the value of b, an increase in the production rate causes the crystal mass distribution to be shifted toward the smaller size crystals. Figure 16 shows the transient response of the fine and coarse fractions of the crystal mass to a step increase in production rate, $T_o/T = 1.25$, for b = 0.2. The fine fraction is here defined as containing all crystals which have a dimensionless size $x < 3$. The coarse fraction consists of all crystals which have a dimensionless size $x > 8$. Thus, the fine and coarse mass percentages are

$$\text{Mass \% Fine} = \frac{\int_0^3 y\, x^3\, dx}{\int_0^\infty y\, x^3\, dx}(100) \tag{113}$$

Figure 16. Transient response of the mass percentage of fine ($x < 3$) and the mass percentage of coarse ($x > 8$) crystals to a step increase in production rate, $T_o/T = 1.25$, for $b = 0.2$

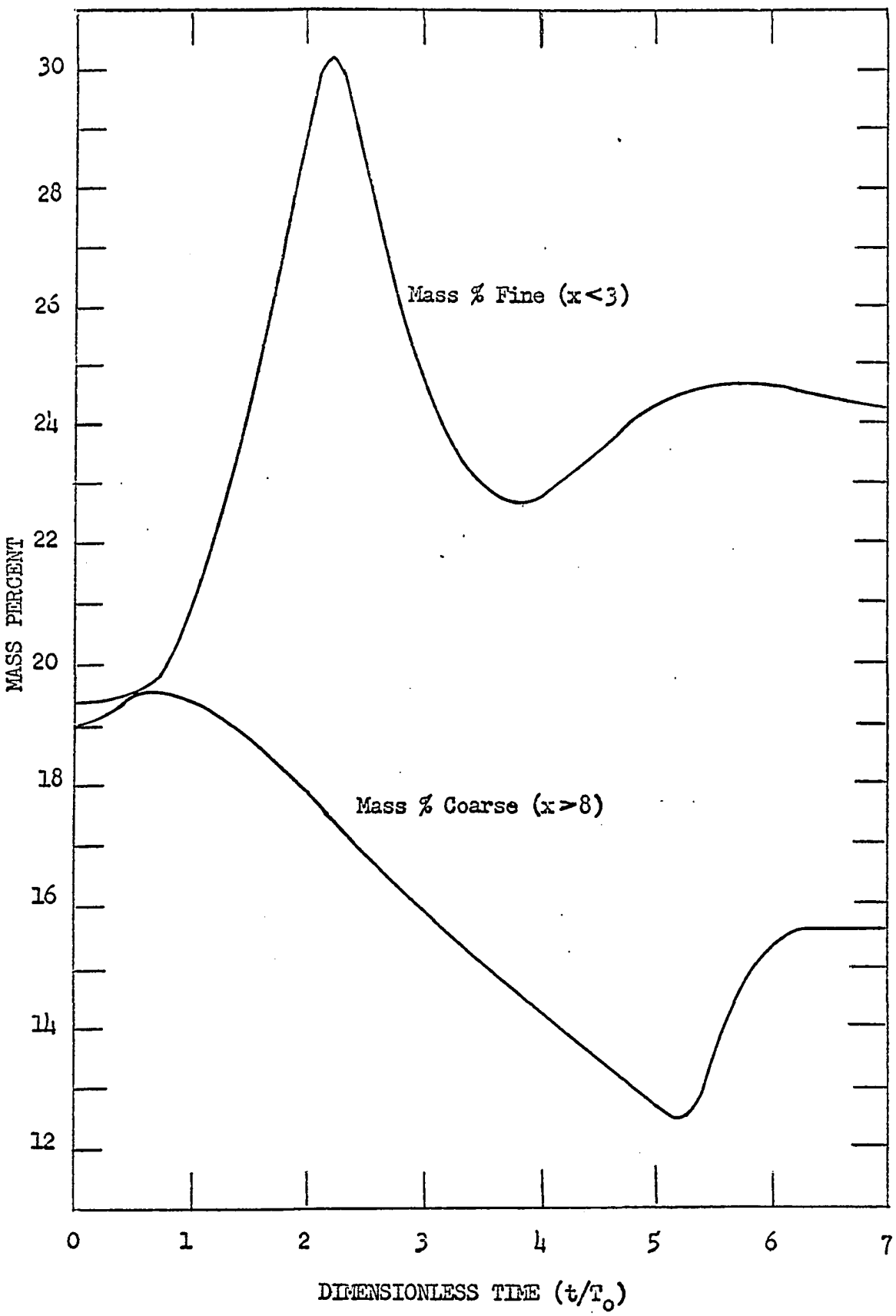
30
28
26
24
22
20
18
16
14
12
MASS PERCENT
Mass % Fine (x<3)
Mass % Coarse (x>8)
0
1
2
3
4
5
6
7
DIMENSIONLESS TIME (t/T$_o$)

$$\text{Mass \% Coarse} = \frac{\int_{8}^{\infty} y\, x^3\, dx}{\int_{o}^{\infty} y\, x^3\, dx}(100) \qquad (114)$$

From Figure 16 it can be seen that approximately equal crystal masses are originally (θ=0) present in the fine and coarse fractions of the mass. After the step change in production rate, seven of the original steady state residence times ($\theta = t/T_o = 7$) are required for the crystal mass to reach a new steady state distribution. At the end of this time, the percentage of the mass contained in the coarse fraction has decreased approximately 3.5%, and the percentage of the mass contained in the fine fraction has increased approximately 5.0%. Hence, an increase in the crystallizer production rate is achieved at the expense of having the crystal mass distribution shifted toward the smaller size crystals.

Unfortunately, there does not seem to be any transient data for growth dependent systems in the literature which are suitable for comparison with the theoretical transient results which have been presented and discussed. However, there are some suitable transient data available for systems which obey McCabe's ΔL Law (5,10,18). These data seem to support the theoretical predictions discussed above.

Step Change in Growth Rate

If the apparent dependency of growth rate on size results from the effect of size on crystal settling velocity, and hence, on crystal-solution relative velocities, the degree of agitation of the crystal

suspension could effect the crystal growth rate. The growth rates of crystals in a vigorously agitated suspension would be expected to be essentially reaction rate controlled, and independent of crystal size or only weakly size dependent. On the other hand, crystals in a mildly agitated suspension could have significantly size dependent growth rates. One might expect, therefore, that a change in the level of agitation of a crystal suspension could change the degree to which the crystal growth rate is influenced by size.

Keeping the production rate constant, and assuming the nucleation and growth kinetics were fourth and first order respectively with regard to the supersaturation, Equations 107 through 109 were numerically solved for a step change in the crystal growth rate. Prior to the step change in growth rate, the crystals were assumed to have a steady state growth rate independent of size (b=0). After the step change, the crystal growth rate was assumed to be size dependent (b = 0.2). The transient response for this type of a change in growth rate might approximate the general transient behavior caused by a sudden reduction in the level of agitation to a crystal suspension.

Figure 17 shows the transient response of the population density. The step change in b causes the supersaturation and the nuclei density to decrease instantaneously. The disturbance in the nuclei density then propogates along the entire size axis, causing transients in the populations densities of all crystal sizes. As time passes, the supersaturation and the nuclei density adjust to new constant values, the transients die out, and the crystal population densities adjust to their new steady

Figure 17. Dimensionless plot of population density versus time for a step increase in b; b=0 → b=0.2

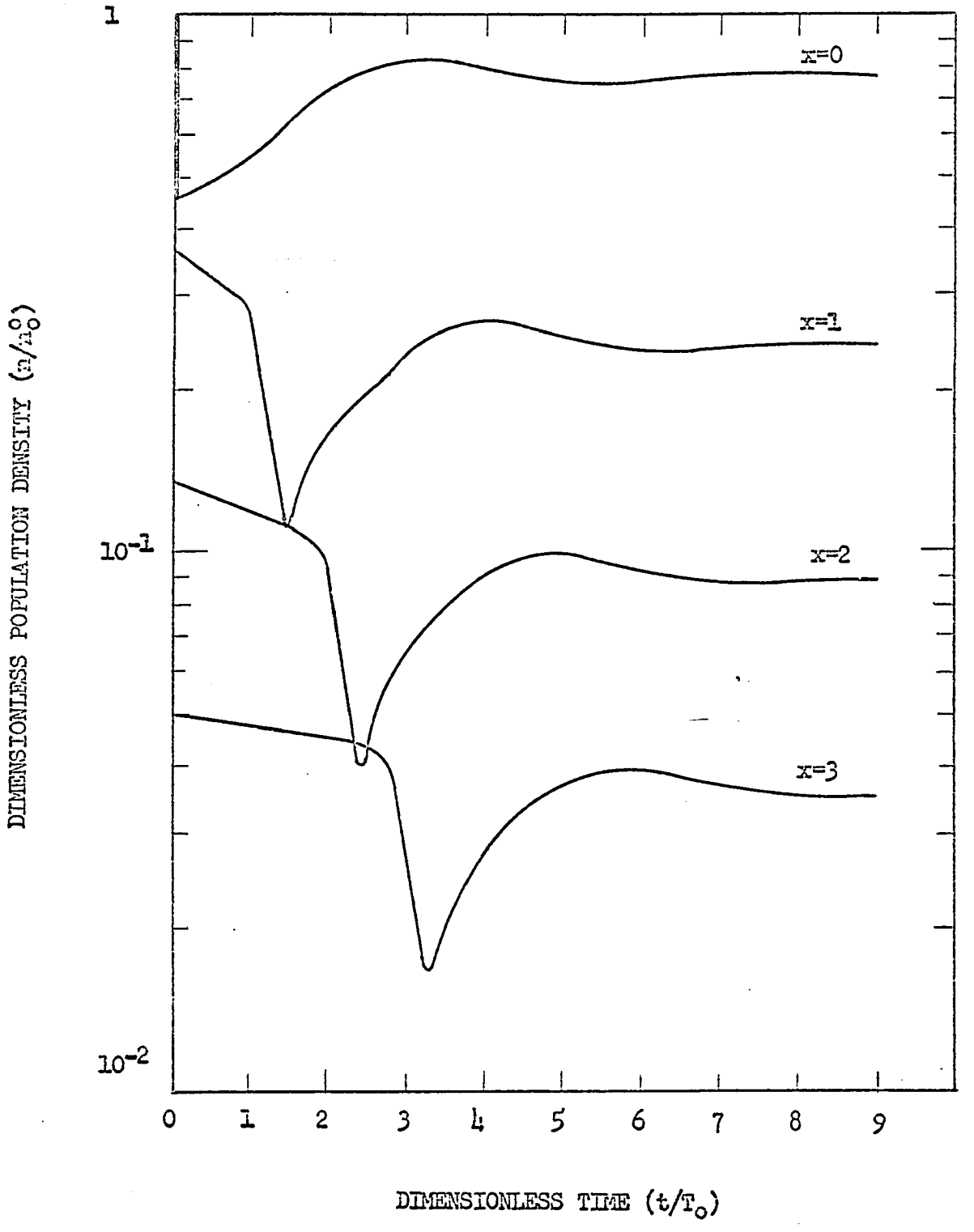
1
10^{-1}
10^{-2}
x=0
x=1
x=2
x=3
0
1
2
3
4
5
6
7
8
9
DIMENSIONLESS POPULATION DENSITY (n/n_o^0)
DIMENSIONLESS TIME (t/T_o)

state values.

Figure 18 shows the original crystal mass distribution for b=0, and the new steady state mass distribution attained after the step change in growth rate to b=0.2. Since the system was constrained to operate at constant mass, the total areas under both curves are the same.

From Figure 18 it can be seen that the step change in growth rate from b=0 to b=0.2 caused the dominant particle size (the particle size at which a mass distribution has its maximum value) to increase from 3.0 to approximately 3.6. From the definition of a population mean and variance,

$$\text{mean} = u = \frac{\int_0^\infty x\, f(x)\, dx}{\int_0^\infty f(x)\, dx} \tag{115}$$

$$\text{variance} = \sigma^2 = \frac{\int_0^\infty (x-u)^2\, f(x)\, dx}{\int_0^\infty f(x)\, dx} \tag{116}$$

where, for the mass distribution, $f(x) = y\, x^3$, the mean and variance were calculated for the two mass distributions. For the original steady state mass distribution (b=0), the integrals of Equations 115 and 116 could be evaluated analytically; the evaluation gave: $u = 4$, $\sigma^2 = 4$. For the final steady state mass distribution (b=0.2), the mean and variance were numerically determined to be: $u = 5.0$, $\sigma^2 = 7.0$. Thus a step change in b from b=0 to b=0.2 increases the dominant particle size and the mean; however, this increase in the dominant particle size and the mean comes about at the expense of a considerable increase in the variance of the mass distribution.

Figure 18. The initial steady state mass distribution for b=0 and the final steady state mass distribution attained after a step increase in b to b=0.2

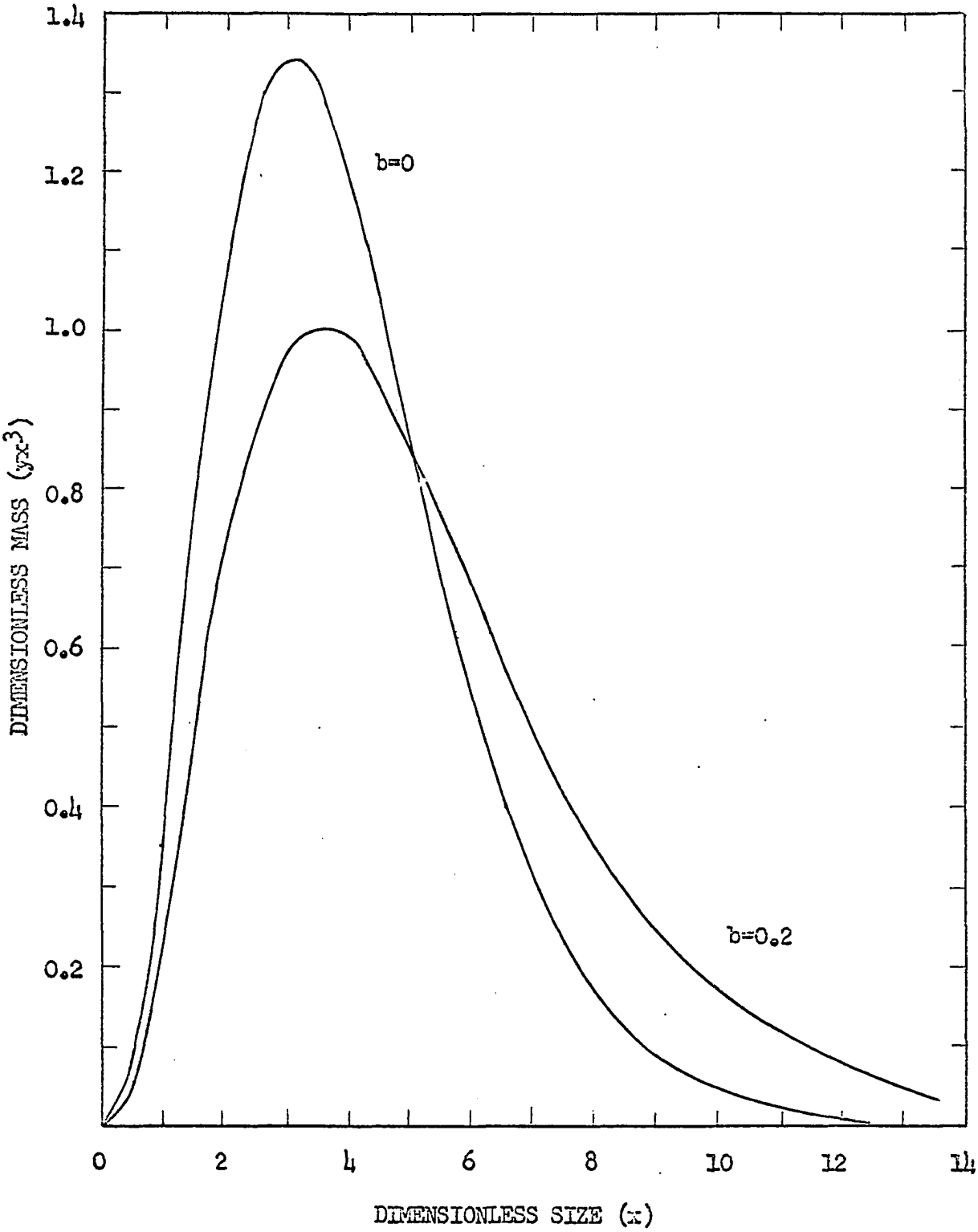
1.4
1.2
1.0
0.8
0.6
0.4
0.2
b=0
b=0.2
DIMENSIONLESS MASS (yx^3)
0
2
4
6
8
10
12
14
DIMENSIONLESS SIZE (x)

RESULTS AND CONCLUSIONS

1. A number of empirical size dependent crystal growth rate models were examined, particularly for their effect on the steady state population density distribution from a continuous, mixed suspension, mixed product removal (CMSMPR) crystallizer. From the examination of these models, criteria were established for a realistic and useful size dependent growth rate expression.
2. Based on these criteria, a new empirical size dependent growth rate model, $r_o = r_o^o(1 + \gamma L)^b$, was proposed. With respect to versatility, continuity, and the convergence of moments of the corresponding population density distribution, the new model is superior to those previously proposed.
3. For three different crystalline materials (alum, tartaric acid, Glauber's salt), experimental CMSMPR crystallizer data indicating possible size dependent growth rates were used to illustrate the application of the model. In each case, it was found that a value of b=0.2 provided a reasonably good fit of the data.
4. Using a general particle population balance equation derived by previous authors, a set of transient equations were derived for predicting the dynamic behavior of the population density distribution. It was assumed thet the crystal growth rate could be expressed as $r = r^o(1 + \gamma L)^b$.
5. The transient equations were solved for the response of the population density distribution to a step increase in production rate. Comparing the transient responses for the size dependent growth rates ($b \neq 0$) with the response for McCabe's ΔL

Law (b=0), it was concluded that the size dependent growth rates had no affect on the general behavior of the population density distribution to a step increase in production rate. The size dependent growth rates simply caused the disturbance in nuclei density to grow through the distribution at a faster or slower rate, depending on whether b was greater or less than zero.

6. It was found that an increase in production rate (decrease in residence time) causes the mass distribution to be shifted in the direction of the smaller crystal sizes.

7. If the dependency of growth rate on size results from the effect of size on the relative crystal-solution velocities, the degree of agitation of the crystal suspension would be expected to effect the crystal growth rate. Hence, it might be possible for a sudden change in the level of agitation to change the degree to which the growth rate is influenced by size. The transient equations were solved for the responses of the population density and mass distributions to a step change in b, $b=0 \rightarrow b=0.2$. This change in b caused the final steady state mass distribution to have a larger dominant particle size, but also a larger variance.

RECOMMENDATIONS

1. Since the value of the growth rate parameter, b, is influenced by the values of n_o^o and r_o^o T_o, it would be advantageous to have a more accurate method of determining these quantities.
2. Very little experimental data are available in the literature for testing the proposed growth rate model. An experimental program could provide the necessary data.
3. Since the suspension density can affect crystal settling velocities, it should be expected to influence the degree to which crystal growth rates are size dependent. An experimental program could provide worthwhile data regarding the effect of suspension density and agitation on systems which exhibit size dependent growth rates.

LITERATURE CITED

1. Behnken, D. W., Horowitz, J., and Katz, S. Particle growth processes. Industrial and Engineering Chemistry Fundamentals 2, No. 3:212. August 1963.

2. Bennett, R. C. Evaporation. 2. Product size distribution in commercial crystallizers. Chemical Engineering Progress 58, No. 9:76. September 1962.

3. Bransom, S. H. Factors in the design of continuous crystallizers. British Chemical Engineering 5:838. 1960.

4a. Bransom, S. H., Dunning, W. J., and Millard, B. Kinetics of crystallization in solution. Part I. Discussions of the Faraday Society 5:83. 1949.

4b. Canning, T. F. and Randolph, A. D. Some aspects of crystallization theory: systems that violate McCabe's delta L law. Unpublished multilithed paper presented at American Institute of Chemical Engineers Mojave Desert regional meeting, Trona, California, October, 1966. Trona, California, American Potash and Chemical Corporation. 1965.

5. Chambliss, C. W. Nucleation and growth kinetics in a cooling crystallizer. Unpublished Ph.D. thesis. Ames, Iowa, Library, Iowa State University of Science and Technology. 1966.

6. McCabe, W. L. and Stevens, R. P. Rate of growth of crystals in aqueous solutions. Chemical Engineering Progress 47, No. 4:168. April 1951.

7. Miers, H. A. The concentration of the solution in contact with a growing crystal. Philosophical Transactions A202:492. 1904.

8. Miers, H. A. and Isaac, F. The refractive indices of crystallizing solutions, with especial reference to the passage from the metastabile to the labile condition. Journal of the Chemical Society (London) 89:413. 1906.

9. Mullin, J. W. Crystallization. London, England, Butterworths. 1961.

10. Murray, D. C. and Larson, M. A. Size distribution dynamics in a salting out crystallizer. American Institute of Chemical Engineers Journal 11:728. 1965.

11. Nielsen, A. E. Kinetics of precipitation. New York, New York, Pergamon Press. 1964.

12. Randolph, A. D. The mixed suspension, mixed product removal crystallizer as a concept in crystallizer design. American Institute of Chemical Engineers Journal 11:424. 1965.

13. Randolph, A. D. Size distribution dynamics in a mixed crystal suspension. Unpublished Ph.D. thesis. Ames, Iowa, Library, Iowa State University of Science and Technology. 1962.

14. Randolph, A. D. and Larson, M. A. Transient and steady state size distributions in continuous mixed suspension crystallizers. American Institute of Chemical Engineers Journal 8:639. 1962.

15. Rumford, F. and Bain, J. The controlled crystallization of sodium chloride. Transactions of the Institution of Chemical Engineers, London 38:10. 1960.

16. Spiegel, M. R. Theory and problems of advanced calculus. New York, New York, Schaum Publishing Company. 1963.

17. Timm, D. C. Crystal size distribution dynamics. Unpublished M.S. thesis. Ames, Iowa, Library, Iowa State University of Science and Technology. 1965.

18. Timm, D. C. and Larson, M. A. Effect of nucleation kinetics on the dynamic behavior of a continuous crystallizer. Unpublished multilited paper presented at American Institute of Chemical Engineers 59th National Meeting, Columbus, Ohio, May, 1966. Ames, Iowa, Department of Chemical Engineering, Iowa State University of Science and Technology. 1966.

19. Ting, H. H. and McCabe, W. C. Supersaturation and crystal formation in seeded solutions. Industrial and Engineering Chemistry 26:1201. 1934.

NOMENCLATURE

A	surface area of a crystal, cm^2
a,b,k	constants used in some crystal growth rate equations
c	concentration of solute component, gm/cm^3
c^*	equilibrium saturation concentration of solute, gm/cm^3
c_i	solute concentration at a crystal-solution interface, gm/cm^3
D	solute diffusivity, $cm^2/sec.$
F	crystallizer feed rate, gm/sec.
ΔG	excess free energy, calories
I^p	p^{th} moment of a population density distribution
K	defined as $\frac{D}{\delta+D/k_r}$
K_1	defined as $n_o^o(L^o)^b \exp[R(L^o)^{1-b}/1-b]$
K_2	defined as $n_o^o(L^o)^{R+1}$
K_3	defined as $\exp(\frac{1}{1-b})$
k_1	defined as $k\, s_o^a$
k_g	constant of proportionality in Equation 15, $cm^4/(sec)(gm)$
k_m	mass transfer coefficient, cm/sec
k_N	nucleation rate constant
k_r	reaction rate constant, cm/sec
k_v	volumetric crystal shape factor
L	characteristic crystal dimension, cm
L_m	size a nucleus grows to in one draw-down time at steady state, cm
M	total mass of crystals in a crystal suspension, gm
$\bar{M}$	solute molecular weight
m	mass of an individual crystal, gm

N	number of crystals
n	population density defined by Equation 19, numbers/cm
$\bar{n}$	point population density per unit volume, numbers/cm/cm^3
n_o^o	nuclei population density at steady state, numbers/cm
'o'	indicates steady state condition when used as a subscript
'o'	refers to nuclei when used as a superscript
R	defined as $1/k_1 T_o$
R'	suspension input or output flow rate, gm/sec
R_g	gas constant, calories/(mole)(°Kelvin)
r	crystal growth rate, cm/sec
r_o^o	steady state nuclei growth rate, cm/sec
s	supersaturation, c-c*, gm/cm^3
$\bar{s}$	supersaturation ratio, $\frac{c}{c^*}$
T	crystallizer draw-down time, sec
T'	suspension temperature, °Kelvin
t	time, sec
V	suspension volume, cm^3
v	relative crystal-solution velocity, cm/sec
W	work of nucleation, calories
x	dimensionless crystal size
y	dimensionless population density
α	exponent in nucleation rate equation
β	defined as α-a
γ	defined as $\frac{1}{r_o^o T_o}$, cm^{-1}
δ	effective film thickness, cm

θ	dimensionless time
ρ	solution density, gm/cm^3
ρ_s	suspension density, gm/cm^3
ρ_c	crystal density, gm/cm^3
σ	surface tension, $calories/cm^2$
ϕ	dimensionless quantity defined by Equation 110

ACKNOWLEDGEMENTS

The author is indebted to Dr. M. A. Larson for suggesting this topic, and for offering ideas and guidance during the course of this research.

The author is especially grateful for the help given to him by his advisor, Dr. J. D. Stevens. Many hours-long sessions were spent with Dr. Stevens who, even when extremely busy with teaching responsibilities, always found enough time to exchange and discuss ideas with the author.

The author also wishes to thank his wife, Joan, for the special help given to him during the preparation of this dissertation.

Support for this research came from an Iowa State University Research Foundation Fellowship, a Minnesota Mining and Manufacturing Company Fellowship, and the Iowa State University Engineering Experiment Station.

APPENDIX

Derivation of the Steady State Distributions for Model-I

If the indefinite integral, $\int \frac{dx}{1+x^b}$, which appears in Equation 61 can be evaluated, an analytical solution can be obtained for the dimensionless population density distributions generated by the Model-I growth rate expression. For many values of b, the indefinite integral can be evaluated.

Consider the right triangle having

$$\text{altitude} = x^{\frac{b}{2}} \tag{117}$$

$$\text{base} = 1 \tag{118}$$

$$\text{hypotenuse} = (1+x^b)^{\frac{1}{2}} \tag{119}$$

Let θ equal the angle between the base and the hypotenuse. Then

$$\tan \theta = x^{\frac{b}{2}} \tag{120}$$

$$x = \tan^{\frac{2}{b}} \theta \tag{121}$$

$$dx = \frac{2}{b} \tan^{\frac{2}{b}-1} \theta \sec^2 \theta d\theta \tag{122}$$

$$1 + x^b = \sec^2 \theta \tag{123}$$

Substituting Equations 122 and 123 into the indefinite integral

$$\int \frac{dx}{1+x^b} = \frac{2}{b} \int \tan^{\frac{2}{b}-1} \theta d\theta \tag{124}$$

Many common tables of integrals show that

$$\int \tan^n x\, dx = \frac{\tan^{n-1} x}{n-1} - \int \tan^{n-2} x\, dx \tag{125}$$

where n is an integer > 1. Hence, if $(\frac{2}{b} - 1)$ is an odd integer n > 1

$$\int \tan^{\frac{2}{b}-1} \theta d\theta = \int \tan^n \theta d\theta = \frac{\tan^{n-1}\theta}{n-1} - \int \tan^{n-2} \theta d\theta \tag{126}$$

$$- \int \tan^{n-2} \theta d\theta = - \frac{\tan^{n-3}\theta}{n-3} + \int \tan^{n-4} \theta d\theta \tag{127}$$

$$\int \tan^{n-4} \theta d\theta = \frac{\tan^{n-5}\theta}{n-5} - \int \tan^{n-6} \theta d\theta \tag{128}$$

$$\vdots \qquad\qquad \vdots$$

$$(-1)^{\frac{n+1}{2}} \int \tan^{n-(n-3)} \theta d\theta = \frac{(-1)^{\frac{n+1}{2}} \tan^{n-(n-2)}\theta}{n-(n-2)} + (-1)^{\frac{n+3}{2}} \int \tan \theta d\theta \tag{129}$$

$$(-1)^{\frac{n+3}{2}} \int \tan \theta d\theta = (-1)^{\frac{n+1}{2}} \ell n \cos \theta \tag{130}$$

Adding Equations 126 through 130

$$\int \tan^n \theta d\theta = \frac{\tan^{n-1}\theta}{n-1} - \frac{\tan^{n-3}\theta}{n-3} + \frac{\tan^{n-5}\theta}{n-5}$$

$$- \cdots + (-1)^{\frac{n+1}{2}} \frac{\tan^{n-(n-2)}\theta}{n-(n-2)}$$

$$+ (-1)^{\frac{n+1}{2}} \ell n \cos \theta \tag{131}$$

or

$$\int \tan^n \theta d\theta = \sum_{j=1}^{\frac{n-1}{2}} (-1)^{j+1} \frac{\tan^{n-(2j-1)}\theta}{n-(2j-1)} + (-1)^{\frac{n+1}{2}} \ln \cos \theta \quad (132)$$

Using Equations 120 and 123, Equation 132 can be written in terms of x

$$\int \tan^n \theta d\theta = \sum_{j=1}^{\frac{n-1}{2}} (-1)^{j+1} \frac{(x^{\frac{b}{2}})^{n-(2j-1)}}{n-(2j-1)}$$

$$+ (-1)^{\frac{n+1}{2}} (-1) \ln (1+x^b)^{\frac{1}{2}} \quad (133)$$

Therefore, from Equations 124 and 133

$$\int \frac{dx}{1+x^b} = \frac{2}{b} \int \tan^n \theta d\theta = \frac{2}{b} \sum_{j=1}^{\frac{n-1}{2}} (-1)^{j+1} \frac{(x^{\frac{b}{2}})^{n-(2j-1)}}{n-(2j-1)}$$

$$+ (\frac{2}{b}) (-1)^{\frac{n+1}{2}} (-1) \ln (1+x^b)^{\frac{1}{2}} \quad (134)$$

Substituting the expression for the indefinite integral from Equation 134 into Equation 61, and using the boundary condition, at x=0 y=1, the analytical solution given by Equation 62 is obtained. If $(\frac{2}{b} - 1)$ is defined as an even integer, m, the above procedure leads to the analytical solution given by Equation 63.

Computer Program

The IBM 360 Model 50 digital computer used in the numerical solution of Equations 107 through 109 was programmed using the FORTRAN statements shown in Figure 19. An identification of the code words used in the FORTRAN program follows.

N	Number of increments in the x-direction
X(J)	A member of the set of values of the independent variable, x. J = 1, 2, ... N
XSQ(J)	A member of the set of values of x^2
XCUB(J)	A member of the set of values of x^3
GP	The growth rate exponent, b
XP1(J)	A member of the set of values of $(1+x)^b$
XP2(J)	A member of the set of values of $(1+x)^{b-1}$
DELTAX	The increment in the x-direction, Δx
T	The independent variable, θ
YN(J)	A member of the set of values of the dependent variable, y, at time θ
DELTAT	The increment in the θ-direction, $\Delta\theta$
YNPI(J)	A member of the set of values of the dependent variable, y, at time $\theta+\Delta\theta$
TMAX	Maximum value of θ after which computation stops
A	A real constant having the value 1.0
B	A real constant having the value -1.0
U	A real constant indicating the fraction of nuclei dissolved. If none of the nuclei formed are dissolved, this has the value 1.0
ORD	Order of the system, $\frac{\alpha-a}{\alpha}$
TRAY	Production rate ratio, T_o/T
JRITE	Machine reference number such that data are printed out only after JRITE increments of $\Delta\theta$

IRITE Machine reference number such that data are printed out only when the index, J, equals the value of IRITE

NRITE A machine integer counter used in a decision statement

KRITE A machine integer counter used in a decision statement

AMASS The value of the numerical approximation of

$$\int_0^\infty y_o \, x^3 \, dx$$

AREA The value of the numerical approximation of

$$\int_0^\infty y_o \, (1+x)^b \, x^2 \, dx$$

ANUC The value of the numerical approximation of

$$\frac{\frac{T_o}{T} \int_0^\infty y_o \, (1+x)^b \, x^2 \, dx}{\int_0^\infty y \, (1+x)^b \, x^2 \, dx}$$

FACT1 Referring to Equation 112, $-\frac{T_o}{T} \frac{\Delta\theta}{2\Delta x}$

FACT2 Referring to Equation 112, $-\frac{T_o}{T} b\Delta\theta$

FACT3 Referring to Equation 112, $-\frac{T_o}{T} \Delta\theta$

FACT 4 The value of the numerical approximation of

$$\frac{T_o}{T} \int_0^\infty y_o \, (1+x)^b \, x^2 \, dx$$

SUM1(J) The numerical approximation of

$$\int_0^{(J-1)\Delta x} y \, (1+x)^b \, x^2 \, dx$$

YSUM1(J) The value of the ordinate $y(1+x)^b x^2$ at position J used in calculating SUM1(J) by means of Simpson's Rule

SUM2(J) The numerical approximation of

$$\int_0^{(J-1)\Delta x} y\, x^3\, dx$$

YSUM2(J) The value of the ordinate $y\, x^3$ at position J used in calculating SUM2(J) by means of Simpson's Rule

Figure 19. Photograph of the computer program used in the numerical solution of Equations 107 through 109

```
      DIMENSION XCUB(1000)
      DIMENSION XP1(1000), XP2(1000),XSQ(1000),YSUM1(1000),YSUM2(1000)
      DIMENSION X(1000), YN(1000), YNP1(1000),SUM1(1000),SUM2(1000)
      READ(1,1) DELTAT,AMASS,AREA,TMAX,GP
    1 FORMAT(1X,5(E14.6))
      READ(1,2) N,JRITE
    2 FORMAT(2(5X,I4))
      WRITE(3,11) DELTAT,AMASS,AREA,TMAX,GP
      WRITE(3,2) N,JRITE
      WRITE(3,3)
    3 FORMAT(21H,5X, 80H SIZE DEPENDENT SIZE DISTRIBUTION DYNAMICS FOR A
     1STEP CHANGE IN PRODUCTION RATE ////)
      A=1.0
      B=-1.0
      U=1.0
      DELTAX=0.05
      T=0.0
      GRO=3.0
      IRITE =5
      TRAY=1.25
      NRITE = 0
      C1=A*EXP(1.0/(1.0-GP))
      X(1)= 0.0
      N1=N-1
      DO 31 J=1,N
      X(J+1)= X(J)+DELTAX
      YN(J)=C1*((1.0+X(J))**(B*GP))*EXP(B*(1.0+X(J))**(1.0-GP)/(1.0-GP))
      IF(IRITE-J)109,28,31
   28 IRITE =IRITE +4
      WRITE(3,30) X(J),YN(J)
   30 FORMAT (5X,F5.2,5X,E13.6)
   31 CONTINUE
      IRITE =5
      WRITE (3,34)
   34 FORMAT (2H )
      PHI  = AMASS/(3.0 *AREA)
      FACT1=((TRAY *DELTAT)/(2.0 * DELTAX))*B
      FACT2 = TRAY *GP *DELTAT *B
      FACT3 = TRAY*DELTAT *B
      FACT4 =  TRAY *AREA
      DO 1000 J=1,N
      XP1(J)=(1.0+ X(J))**GP
      XP2(J)=(1.0 +X(J))**(GP -1.0)
      XSQ(J)= X(J)*X(J)
 1000 XCUB(J)= XSQ(J)*X(J)
      ANUC=1.0
      IT=0
      YNP1(1)= U *ANUC**3
      YNP1(N1=FACT1*PHI*XP1(N)*2.0* (YN(N)-YN(N1)) *(1.0 +FACT2*PHI*
     1XP2(N)+FACT3)*YN(N)
      DO 48 J=2,N1
      YNP1(J)=FACT1 *PHI *XP1(J)*(YN(J+1)-YN(J-1))+(1.0+FACT2*PHI*
     1XP2(J)+FACT3)*YN(J)
      SUM1(1)=0.0
      KRITE = 1
      DO 56 J=1,N
      YSUM1(J)= YNP1(J)*XP1(J)*XSQ(J)
```

```
      IF(KRITE-J)109,56,58
      KRITE =KRITE +2
      SUM1(J)= (DELTAX/3.0)*( YSUM1(J-2)+4.0 *YSUM1(J-1)+YSUM1(J) ) +
     1 SUM1(J-2)
      CONTINUE
      PHI1 = AMASS/(3.0 * SUM1(N))
      ANUC1 =(FACT4/SUM1(N))
      IF(ABS(PHI1-PHI)-0.01)74,62,62
      PHI =PHI1
      ANUC = ANUC1
      IT= IT+1
      IF(IT-10)45,45,66
      YTEST= FACT1* PHI *XP1(1)*2.0 *( YN(2)-YN(1)) + (1.0 +FACT2*PHI*
     1XP2(1)+FACT3)*YN(1)
      WRITE (3,70)
   70 FORMAT(21H, 26HO NEWS, ABS(PHI1-PHI) FAILED TO CONVERGE TO
     1WITHIN 0.01 IN 10 ITERATIONS3 ////)
      WRITE(3,72) IT,YTEST,YNP1(1),PHI,ANUC,T
   72 FORMAT ( 5X,I4,4(5X,E13.6),5X,F6.3)
      GO TO 105
      I =T* DELTAT
      PHI = PHI1
      ANUC= ANUC1
      NRITE =NRITE +1
      IF(JRITE - NRITE) 109,82,79
      DO 80 J=1,N
      YN(J) =YNP1(J)
      GO TO 44
      NRITE = 0
      YTEST= FACT1* PHI *XP1(1)*2.0 *( YN(2)-YN(1)) + (1.0 +FACT2*PHI*
     1XP2(1)+FACT3)*YN(1)
      WRITE(3,85) T,IT,YTEST,YNP1(1),PHI,ANUC
      FORMAT (/////, 5X,F6.3,15X,I4,4(5X,E13.6)//)
      DO 87 J=1,N
      YN(J)= YNP1(J)
      KRITE =3
      SUM2(1)= 0.0
      DO 101 J=1,N
      YSUM2(J) = YN(J) * XCUB(J)
      IF(KRITE -J)109,92,101
      KRITE =KRITE + 2
      SUM2(J)= (DELTAX/3.0)*(YSUM2(J-2)+ 4.0* YSUM2(J-1)+YSUM2(J)) +
     1 SUM2(J-2)
      IF(IRITE-J)109,96,101
      IRITE =IRITE +4
      PERCT =(100.0 * SUM2(J) )/AMASS
      IF( NI -J)102,99,99
      WRITE (3,100) X(J),YN(J),PERCT,SUM2(J),YSUM2(J)
  100 FORMAT(5X,F6.2,4(5X,E13.6))
  101 CONTINUE
      IRITE = 5
      KRITE = 3
      IF(TMAX-T) 105,105,44
      WRITE (2,106) T,PHI,ANUC
  106 FORMAT (6X,3E14.6)
      WRITE (2,108) (YN(J),J=1,N)
  108 FORMAT(1X,5E14.6)
  109 STOP
  110 END
```